Impact of Mobility Design on Network Connectivity Dynamics in Urban Environment

Younes Regragui, Najem Moussa

Impact of Mobility Design on Network Connectivity Dynamics in Urban Environment

Younes Regragui[a,*], Najem Moussa[b]

[a]*LAROSERI, Department of Computer Science, Chouaib Doukkali University, El Jadida 24000, Morocco.*
[b]*Faculty of Sciences, Mohammed V University in Rabat, Rabat, Morocco.*

Abstract

Vehicular ad hoc networks have emerged as a promising research area for enabling various types of applications. However, VANETs are facing the biggest challenges in providing reliable communications due to unstable network connectivity caused by vehicle mobility. Several efforts have been carried out to analyze this problem. However, these efforts ignore the impact of intelligent mobility designs. This work highlights the relationship between intelligent mobility for transportation systems and connectivity dynamics. For this purpose, a framework of different mobility models is proposed based on the cellular automata (CA) approach to simulate vehicles mobility in a Manhattan two-dimensional network of roundabouts. To take into account intelligent aspects of mobility for drivers, a centralized path planning strategy based on the Bellman–Ford algorithm analyzes the travel time at road segments to provide the shortest paths for vehicles. Besides, we categorize three mobility models: In the first mobility model, vehicles are assigned the shortest paths in real-time with a periodic update. Each shortest path is defined as a set of turning movements (i.e., right, left, straight, ...), where each turning step represents the driver's decision at the next roundabout. At roundabouts, vehicles follow priority rules to avoid conflict with other traffics. The second mobility model is similar to the first one, but vehicles do have not the possibility to update their assigned shortest paths. The third model extends the first one by using traffic lights instead of priority rules at roundabouts. Extensive simulations based on both generated mobility traces and NS-2 analyze both network connectivity and reliability under several effective factors, including vehicles' mobility model, vehicles' speed, vehicles' density, transmission range, and RSUs deployment strategy in terms of RSUs' position and number. Several performance metrics of interest are introduced (such as packet delivery ratio, paths length, link duration, and end-to-end delay). The simulation results show that both the network performance and connectivity condition are sensitive to multiple factors, which reflect the V2V and V2I communications under varying conditions.

Keywords: Intelligent mobility, Network connectivity, Traffic state, Topology condition, Transportation systems, VANETs, Wireless communications

1. Introduction

The last decade has seen a rapidly increasing development in Vehicular Ad Hoc Networks (VANETs) because VANETs are considered to be a promising concept for enabling various types of applications and services for intelligent transportation systems (ITS) [1] (i.e., avoiding traffic congestions, providing intelligent traffic signaling, collision warning, cooperative incident management, speed violation detection, and many more [2, 3]). In this regard, VANETs involve the use of vehicle-to-vehicle (V2V) communications and vehicle-to-Infrastructure (V2I) communications for providing a relay of data information to distant nodes

*Corresponding author: Y. Regragui
Email addresses: regragui.y@ucd.ac.ma (Younes Regragui), najemmoussa@yahoo.fr (Najem Moussa)

via multi-hop communications [4]. Despite the benefits of VANETs networks, various challenges may impact the exchange of communications between source and destination nodes, including vehicles' density, vehicles' mobility, routing overhead, and so on. However, the perturbation in the network connectivity due to vehicle mobility is considered to be among the most challenging problems [5]. In other words, the frequent change in network connectivity due to vehicle mobility is the main responsible for wireless links failure [6], and thus the network becomes unable to provide efficient services for drivers, especially in the case of emergencies.

Over the last few years, simulation tools and mobility modeling for vehicular traffic have attracted the great attention of researchers and become widely adopted to handle this critical problem under varying mobility scenarios. Indeed, several mobility models have been proposed to analyze and make a deep understanding of this critical problem. For instance, some researchers adopt mesoscopic mobility modeling to analyze connectivity in VANETs either in such scenarios of Traffic-Centric [7] or either by adopting a macroscopic mobility modeling to provide more realistic characteristics to vehicular network evaluation [8]. Unlike macroscopic and mesoscopic mobility modeling, microscopic mobility modeling provides higher fidelity and it is widely adopted by researchers to model vehicular mobility scenarios and to exploit them in solving the connectivity issues in VANETs. For instance, it can be adopted to estimate vehicles' current positions and calculate the connectivity probability based on the vehicle's individual information recorded at the intersection [9]. Some researchers tried to adopt microscopic mobility modeling to analyze V2V connectivity dynamics by considering dependent metrics such as vehicle's speed, vehicle's density and network parameters [10]. Other attempts of researchers are oriented to adopt microscopic mobility modeling to analyze connectivity characteristics in large-scale VANETs scenarios [11–13].

The importance of mobility modeling has encouraged researchers to combine macroscopic mobility modeling and real data recorded at transportation systems to introduce realistic synthetic datasets. For instance, to evaluate networking scenarios, a combination between microscopic mobility and a realistic dataset of traffic could be a good solution to generate a large-scale synthetic trace of vehicular traffic [14]. Synthetic mobility was also adopted to study and unveil the characteristics of network topology in real large-scale urban vehicular scenarios, especially in the case of networking solutions that relay on direct communication (e.g., channel access management or cooperative awareness), or either those relay on multi-hop forwarding (e.g., delay-sensitive information propagation, connected routing, or cooperative autonomous driving) [11].

Most of the proposed studies on vehicular mobility modeling to analyze the network connectivity have not analyzed the network connectivity sufficiently based on efficient performance metrics and varying evaluation scenarios, also these researches neglect the impact of intelligent mobility aspects, which becomes a necessity for ITS.

In this paper, we first focus on how the role of mobility designs can impact network connectivity dynamics, especially since mobility design is assumed to have effects on the way the vehicles are distributed in the network area. In other words, at each time step, the network topology may reflect a picture of how vehicles are distributed in the network area under constraints of both drivers' decision-making behavior and traffic state. This leads us to think more about the role of mobility design in impacting network connectivity. Motivated by limitations of previous research in this trend, particularly the effects of intelligent mobility on network connectivity, which is become an emergency. Our efforts conducted us to think about joining microscopic mobility modeling based on the cellular automata (CA) technique for representing realistically as possible the aspects of vehicular mobility. Accordingly, several realistic aspects of vehicular mobility are included based on microscopic rules, as follows:

- Real roundabout design is adopted, where the adopted roundabout design is based on the real-world roundabout.
- Vehicle speed limit inside road segments (or maximum speed V_{max}).
- Vehicle speed limit inside roundabouts (or maximum speed $V_{max_{ra}}$).
- Priority rules at roundabouts when traffic lights are not used, including priority rules at entry and exit legs of the roundabout.
- Acceleration and deceleration behaviors.

- Vehicles should make slow down followed by a stop when traffic lights are red.
- Vehicles travel based on their assigned pairs of origins and destinations.
- Vehicles mobility is provided in terms of safety gaps.
- Realistic traffic light duration cycle.
- Drivers can make a right turning without entering the roundabout.
- Drivers can make a U-turn at the roundabout when the destination is located at the opposite line.
- Drivers can follow the shortest paths in real-time in terms of travel time to reach the destination.

Moreover, the proposed mobility framework provides intelligent aspects of vehicular mobility for drivers, where vehicles are assigned the shortest paths based on a centralized path planning strategy to provide re-routing of vehicles during their travel. To minimize the travel time on the road, the path planning strategy uses a distributed traffic information collection mechanism by collecting periodically travel time at the level of each road segment. Based on the collected traffic information, the Bellman–Ford algorithm is processed next to find the shortest paths between origin–destinations pairs in terms of travel time (see Fig. 1).

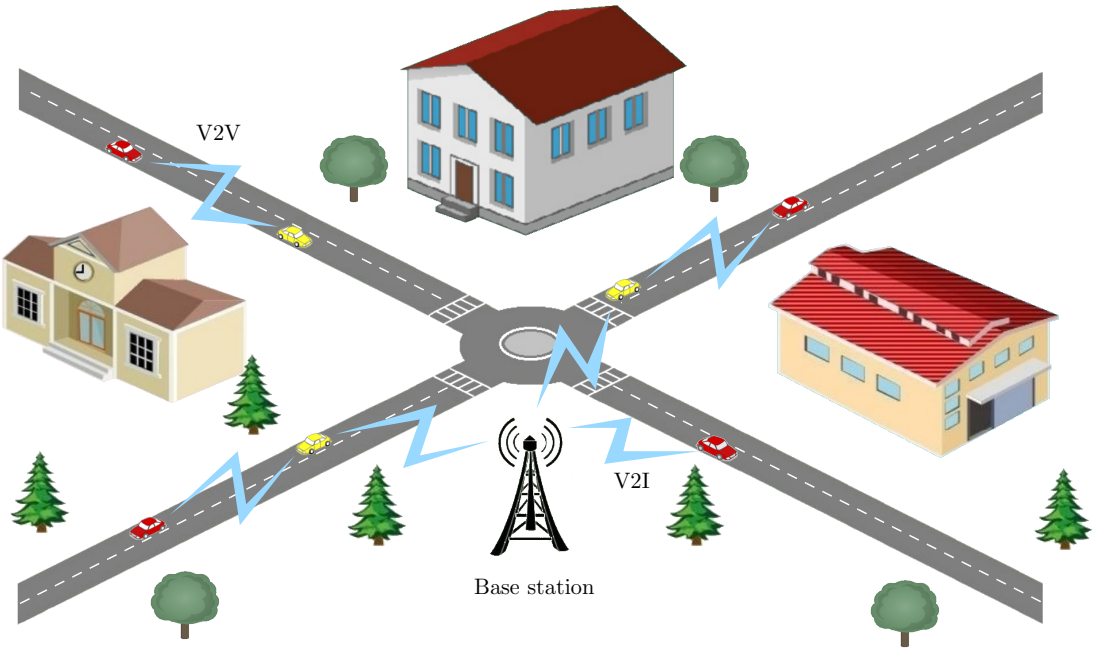

Fig. 1. Illustration of V2V and V2I communications in an urban environment.

Secondly, based on the ability of our proposed mobility framework to simulate vehicular traffic in a large-scale urban environment, we aim to answer the main question about the relationship between connectivity dynamics and the reliability of the VANET network. Indeed, the contributions of this work are threefold:

1. A mobility framework is proposed to simulate traffic scenarios in a large-scale urban environment, including various mobility models.
2. The transportation system is evaluated for various performance metrics relative to traffic dynamics, including traffic flow, average speed, and travel time. The purpose of this evaluation is to identify and understand different traffic states while varying the traffic parameters, including vehicles' density and mobility design.

3. We analyze the network reliability and connectivity dynamics in a large urban environment by taking into account several effective factors on the vehicular traffic and network behavior. For this purpose, we consider several metrics to monitor the effectiveness of network performance and connectivity dynamics, including packet delivery ratio, end-to-end delay, path length, and link duration. The considered effective factors and parameters for analyzing the network behavior are listed as follows:
   a. Vehicle mobility model, including three different mobility models that are based on the proposed path planning strategy.
   b. The transmission range, which is expected to help us to depict an idea about network connectivity in terms of established paths, wireless links' duration, and end-to-end delay.
   c. Also, we shed light on the effects of RUSs' deployment strategy as a function of RSUs' position and number. The deployment of RSUs is intended to increase the network coverage. The proposed RSUs deployment strategy provides an uniform placement of RSUs in the network area.

The rest of the paper is organized as follows. We first review the related work in section 2. Next, we describe the proposed mobility framework in section 3. In section 4, we describe the adopted mobility scenarios, network model, performance metrics, and adopted parameters to analyze connectivity and network reliability. Section 5 presents the simulation results and discussions. Finally, in section 6, the paper is concluded.

2. Related work

Over the last few years, the research community has proposed several mobility models to analyze and evaluate network connectivity dynamics under varying vehicular traffic scenarios. The common purpose for all proposed works is to introduce realistic simulation tools capable of simulating real traffic, and therefore analyze and evaluate networking issues, among them the connectivity dynamics. Table 1 summarizes different features of the proposed solutions found in the literature. The problem of network connectivity has been studied extensively in terms of varying effective factors such as mobility, speed, density, and other parameters. This includes studies based on one-dimensional, multi-lane and square grids scenarios, probability theory-based models, Markov Chain based models, graph theory-based models and so on [24–32]. All these studies prove that the connectivity problem in VANETs is still a challenging problem that depends on different perspectives of both vehicular traffic and networking settings, and therefore this encouraged us to think about the need for more realistic mobility models as the main entry to analyze network connectivity dynamics.

In the last few years, there have been many attempts to propose mobility models that can simulate real traffic as realistically as possible. One salient purpose is to analyze network connectivity and reliability under realistic traffic scenarios. For instance, in [7], a mesoscopic vehicular mobility model in a multilane highway with a steady-state traffic flow condition was introduced to analyze network connectivity based on the traffic-centric distribution of both spatial and expected per-hop progress. Accordingly, different inter-vehicle distance distributions are utilized. In [33], a mesoscopic model of urban traffic to analyze information dissemination in urban VANETs was proposed based on an agent-based model (ABM). It focuses on characteristics of some spatial aspects of the information spreading process.

Other works are based on macroscopic mobility modeling instead of mesoscopic mobility modeling, for example, in [8], to provide more realistic aspects to the evaluation approach of vehicular networks, a novel macroscopic mobility model was introduced based on a realistic vehicular mobility trace. It considers a generic origin–destination model by applying statistical inference techniques. For this purpose, it considers traffic behavior in terms of departures and arrivals in space, departures in time, total traveled distance, and total travel time, which together describe the origin–destination behavior. In [15], to investigate the connectivity probability for VANET freeway traffic, a discrete bidirectional two-lane freeway model scenario at the macroscopic level was proposed. This last allows partitioning of time in a way that one vehicle takes a one-time unit to travel through one cell at free-flow speed. Based on this model, the network connectivity was analyzed according to a set of parameters, such as vehicles flow, path loss exponent, the communication radius, the message size, and the data rate.

Table 1. A comparison between different studies in the literature based on a set of features.

Reference	Study	Type of scenario	Connectivity metrics	Realistic mobility features	Impact of intelligent mobility on connectivity	Level of connectivity analysis	Type of model
Proposed	Mobility +connectivity	Large-scale	PDR per hop+path length+end-to-end delay +link duration	✓	×	high-detail	Microscopic
[7]	Mobility +connectivity	Multilane highway	Expected number of hops+distribution of successful multihop	×	×	medium	Mesoscopic
[8]	Mobility	large-scale	-	✓	×	×	Macroscopic
[15]	Mobility + connectivity	Freeway scenario	Connectivity probability	×	×	medium	Macroscopic
[16]	Mobility +Connectivity	Highway	Link duration +number of neighbors	✓	×	medium	Microscopic
[11]	Mobility +connectivity	Large-scale	Component level+network level +node level	✓	×	high	Microscopic
[17]	Mobility +Connectivity	Large-scale	Reachability +transitive closure	✓	×	low	Microscopic
[18]	Mobility +connectivity	Large-scale	component speed +component size	✓	×	medium	Microscopic
[19]	Mobility +Connectivity	Large-scale	Probability of connectivity +data forwarding time	×	×	high	Theoretical
[12]	Mobility	Large-scale	-	✓	×	×	Microscopic
[20]	Mobility	Large-scale	-	✓	×	×	Microscopic
[21]	Mobility +Connectivity	Large-scale scenario	Link duration+nodal degree +number of connected components	✓	×	low	Microscopic
[22]	Mobility +Connectivity	Large-scale	Edge percentage+Diameter +nodes' degree+Normalized transitivity+Betweenness centrality	✓	×	medium	Microscopic
[23]	Mobility +Connectivity	Crossing	Path reachability+link duration+re-healing period time	✓	✓	medium	Microscopic
[10]	Mobility +connectivity	Highway	Communication duration +connectivity probability	✓	✓	medium	Microscopic

However, both macroscopic and mesoscopic mobility modeling provide less fidelity when the matter is related to realistic mobility as compared with microscopic mobility modeling, which is widely adopted by researchers to introduce varying vehicular mobility scenarios. Due to its main advantage in providing both discrete-time and space, microscopic mobility models allow capturing several characteristics of traffic flow at a microscopic level such as acceleration/deceleration, cars following each other, slow down anticipations, and so on. These advantages are exploited to help in building realistic scenarios and therefore help in analyzing efficiently the connectivity issues in VANETs. For example, in [34], VehILux vehicular mobility model which is based on real traffic counting data was introduced to provide mobility traces at the microscopic level. It relies on real information about the country of Luxembourg and geographical information about different types of areas: residential, industrial, commercial, and other services. It considers two types of traffic: The first one consists of the vehicle flows provided by traffic counting devices. This data is provided by the Luxembourg Ministry of Transport. The second source of information is the OpenStreetMap project which provides detailed information about the road network and the zones of activity in the country. VehILux is coupled with the microscopic simulator of urban mobility (SUMO) to produce realistic vehicular traces.

To analyze and understand the dynamics of the network topology characteristics since this one determines the level of fidelity to provide reliable communications for many applications over VANETs, especially those based on real-time. In [21], a preliminary analysis for VANET network topology characteristics for low and high traffic density was proposed. Accordingly, the integration of real-world buildings and obstacles along with the propagation environments and measured data from the California Performance Measurement System (PeMS) database into a microscopic mobility model was realized to obtain realistic traffic flows. Several performance metrics were introduced to analyze connectivity dynamics, including link duration, nodal degree, and the number of connected components. In [16], an integration between real-world road topology and real-time data extracted from the Freeway Performance Measurement System (PeMS) database was realized based on a microscopic mobility model to generate realistic traffic flows along the highway. In [11], a synthetic mobility was also adopted to study and unveil the characteristics of network topology in real large-scale urban vehicular scenarios, especially in the case of networking solutions that relay on direct communication (e.g., channel access management or cooperative awareness), or either those relay on multi-hop forwarding (e.g., delay-sensitive information propagation, connected routing, or cooperative autonomous driving). For the same purpose, in [17], authors proposed realistic mobility in urban settings that exhibit an unprecedented combination of dependability, scale, and generality of vehicular mobility. They adopted a realistic dataset at a microscopic-level of urban road traffic in Cologne, Germany; the dataset contains positioning information on individual vehicles every second, for a full day. This information is used to select a random subset of vehicles and a subsample of their trajectories at periodicities varying between 10 and 300 s. Thereafter, the subsampled trajectories are calibrated using both a proposed methodology and a state-of-the-art solution proposed in [35] to generate new trajectories with high accuracy.

The main advantage of these works above is that they combine the use of real traces and microscopic simulation tools of vehicular traffic such as SUMO due to its efficiency to build realistic traffic scenarios. However, this combination is constrained by the degree of calibration of collected mobility traces for SUMO environment by kipping the original behavioral rules on the road.

The problem of unstable network connectivity has attracted the attention of another class of researchers to adopt mathematical approaches to analyze the impact of vehicle mobility on network connectivity dynamics based on large-scale scenarios. For example, the authors in [18] analyzed the relationship between the mobility and connectivity of VANETs based on a large-scale real-world urban mobility trace data set. Accordingly, they discovered that there exists a dichotomy in the relationship between component speed and size. This dichotomy indicates that mobility destroys the connectivity when the speed becomes higher than a specific threshold; otherwise, it has no apparent impact on connectivity. Based on this observation, they proposed a mathematical model to characterize this relationship, which agrees well with empirical results. In [19], the authors introduced a theoretical method to investigate four connectivity properties in an urban road scene, including the possibility, data forwarding time, link forwarding capability, and packet error rate. The experimental results demonstrated that the model is suitable for a vehicle network with infrastructure in an urban scene, and it can be used to accurately evaluate the network connectivity of a highly dynamic large-scale heterogeneous vehicle network.

Regardless of significant attempts to analyze the relationship between mobility and connectivity by adopting some key metrics such as data forwarding time and link forwarding capability or some effective factors such as vehicle speed. However, none of these approaches have incorporated accurate aspects of realistic vehicle mobility, including the influence of the user behavior [36].

Other contributions about vehicular mobility modeling can be found in the literature. These works focus on re-routing capabilities as an important aspect of intelligent transportation systems (ITS), which is capable of providing more flexibility of traffic flow for drivers when the matter is related to the need to avoid traffic congestion or unexpected traffic jams. In [12], a vehicle route planning based on the macroscopic motion was proposed to optimize vehicle route and speed simultaneously using both traffic data and vehicle characteristics to improve fuel economy for a given expected trip time. For this purpose, a simulation model, combining a traffic model based on SUMO (Simulation of Urban Mobility) with a Simulink powertrain model, is developed to validate the proposed method. In [20], another vehicle route planning based on an efficient real-time information-sharing mechanism to achieve the real-time traveling time estimation and dynamic path planning. It uses a sharing mechanism based on a distributed transportation system with RSUs, which has lower computing complexity and less redundancy. This method is evaluated With VanetMobiSim, a simulator at both macroscopic and microscopic levels. In [22], to provide a realistic analysis of both mobility of vehicles and network connectivity, an automatic vehicle re-routing mechanism is proposed based on graph theory concepts to re-compute routes in front of specific traffic conditions (e.g., traffic jams). Based on the SUMO simulator and previous constraints, realistic mobility is generated based on a real map, where vehicles are allowed to change their routes during their trips dynamically and periodically according to the current traffic state.

Regardless that all methods above adopt re-routing capabilities based on the Dynamic User Assignment tool called Duarouter provided by SUMO; however, the Duarouter is still naive and it is not capable to guarantee that a vehicle always chooses the "cheapest" route as it is based on a probabilistic approach. On the other hand, most introduced works have not analyzed explicitly the network connectivity problem in VANETs, which indicates a limitation in depicting the relationship between the re-routing mobility design and network connectivity dynamics.

Very recently, some researchers focussed their attention on how intelligent mobility designs can impact network connectivity. For example, in [23], authors analyzed the impact of intelligent traffic lights on VANETs connectivity based on several performance metrics, including reachability, connection duration, and re-healing time. The findings are compared with those of classical scenarios: synchronized traffic lights and no traffic lights. In [10], to analyze V2V connectivity dynamics among V2V, microscopic mobility and lane changing decision model were introduced using an adaptive cursive control mechanism and recurrent neural network. Based on an analytical model, the authors provided a framework for examining the impact of mobility via multiple metrics such as vehicle speed, acceleration/deceleration, safety gap, vehicle arrival rate, vehicle density, and network metric data delivery rate for characterizing the VANET connectivity of the proposed network. For this purpose, the proposed framework provides a generation of mobility trace as input for two different simulators, such as (SUMO) and network simulator (NS-2).

However, these works considered only simple scenarios to analyze network connectivity dynamics, which is considered insufficient to give us a clear picture under the assumption that established paths length may be too short, which is not sufficient to reflect realistic challenges for multi-hops V2V and V2I communications.

In reference to the relevant works discussed above, we conclude that the attention has been highly devoted to mobility design more than connectivity analysis, while we still lack sufficient approaches to analyze network connectivity condition more carefully, especially under large-scale scenarios and the emergence of intelligent mobility. For example, by adopting convenient performance metrics and realistic traffic scenarios, the findings are expected to give us an extra detailed picture of network connectivity dynamics. In fact, the network connectivity depends to many effective factors, such as mobility design, vehicles' speed, vehicles' density, and network parameters. Regardless that researchers focussed on some important components such as driver behavior via re-routing capabilities or changing speed; however, we still lack discovering how intelligent mobility can impact network connectivity, especially with the highly increasing interest in intelligent transportation systems (ITS).

In this work, our goal is to fill this gap by joining microscopic mobility modeling to perform realistic

mobility characterization with re-routing capabilities based on a centralized path planning strategy to make deriving more intelligent on the road. Based on the proposed mobility framework, varying large-scale scenarios are simulated and mobility traces are generated for the NS-2 simulator (see Fig. 10) to perform plenty of network connectivity analysis based on several performance metrics.

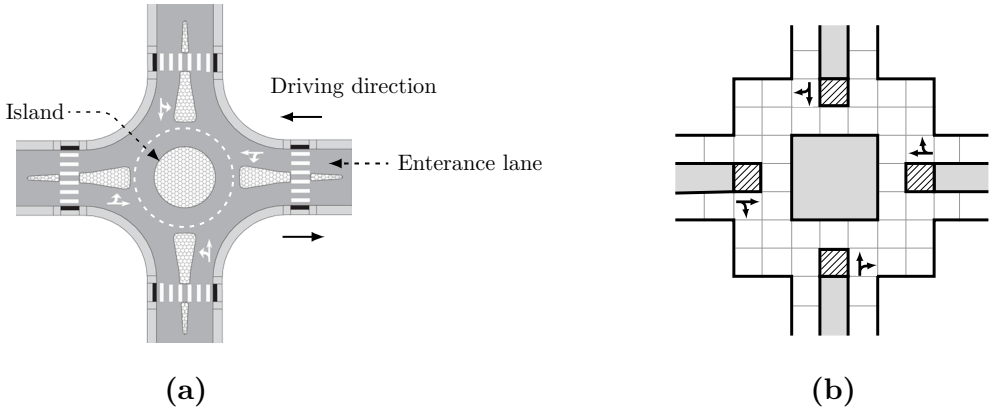

Fig. 2. Illustration of the proposed CA roundabout model based on a real-world roundabout.

3. Model Descriptions

In this section, we provide a detailed description of the proposed mobility framework that includes three mobility models, which are based on the Cellular Automata (CA) concept. All proposed mobility models share the same core, except for some functionalities. The proposed mobility models are described as follows:

1. The first mobility model implements vertical and horizontal streets like a two-dimensional Manhattan grid, but at each intersection, a roundabout is deployed instead of a crossing. This model provides real-time path planning based on a shortest path algorithm. Accordingly, it allows a vehicle A to get a shortest path between a source and destination. The obtained shortest path represents a movement trajectory (a set of turning steps at roundabout). The calculation of shortest paths is based on the travel time in each road segment. When vehicle A reaches an intersection (roundabout), it can update its trajectory depending on the traffic state in terms of travel time, where a new shortest path will be calculated and assigned to vehicle A.
2. The second mobility model is similar to the first one, but vehicles can not update their trajectories when they reach an intersection. This means that they keep the initially assigned shortest path until they reach their destinations.
3. The third model extends the first one by using traffic lights instead of priority rules at the roundabouts.

3.1. Two-dimensional Cellular Road Structure

We consider a Cellular Automata (CA) model described in the two-dimensional system. The underlying proposed structure is a $L \times L$ cell grid, where L is the system size. The proposed structure is similar to a two-dimensional Manhattan grid where all streets are two-way, with one lane in each direction. At each intersection between vertical and horizontal streets, a roundabout is used instead of a crossing to manage vehicular traffic and reduce conflicting scenarios between vehicles. The distance between each pair of roundabouts is configured with a predefined value at the beginning of simulation (see 2). Each cell can either be empty or occupied by exactly one vehicle. The length of a single cell is set to 7.5 m in accordance with the NaSch model [37]. The vehicles move within the simulation area without periodic boundary conditions and without using a changing lane model. In each simulation setup, vehicles are either eastbound

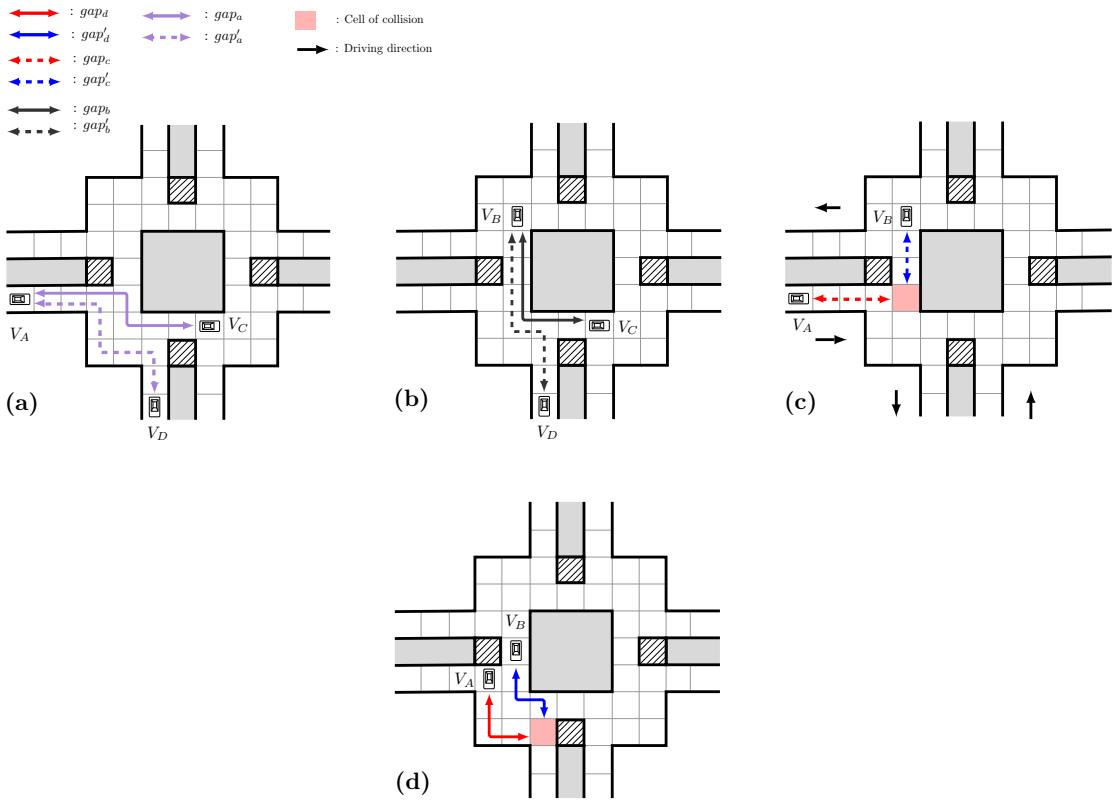

Fig. 3. Illustration of different gaps used to manage priority between entering vehicles, circulating vehicles and exiting vehicles inside the roundabout.

or westbound, or southbound or northbound. When a vehicle n enters the roundabout, it can change its direction depending on the next road segment in its assigned shortest path based on the Bellman–Ford algorithm (see Fig. 4 and Fig. 8). The global density is defined by $\rho = N/L^2$. To keep the same vehicles' density in the traffic system, each vehicle that reached its destination will be removed and replaced by another one with a new random source and destination. At each discrete time step $t \longrightarrow t+1$, the vehicles' movement in terms of speed v(t) for each vehicle n is updated in parallel according to the following rules:

- Acceleration outside the roundabout.
  $v_n(t+1) = min(v_n(t)+1, v_{max})$, where v_{max} is the maximum speed and $v_n(t)$ denote the speed of the vehicle.
- Acceleration inside the roundabout.
  $v_n(t+1) = min(v_n(t)+1, v_{max_{rp}})$, where $v_{max_{rp}}$ is the maximum speed inside the roundabout.
- Deceleration.
  $v_n(t+1) = min(v_n(t), d_n(t))$ (resp. $v_n(t+1) = min(v_n(t), gap_c)$), where $d_n(t) = x_{n+1}(t) - x_n(t) - 1$ denotes the number of empty cells in front of the vehicle n between two successive vehicles or between the vehicle and the last cell in the lane (gap_c).
- Randomization, braking : $v_n(t+1) = min(v_n(t), 0)$.
- Vehicle motion.
  Each vehicle will move according to its new speed.

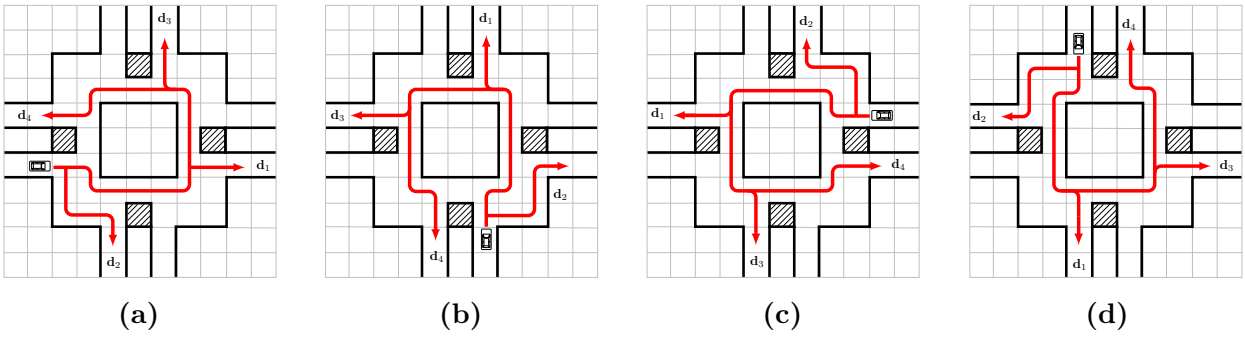

Fig. 4. Illustration of different driving directions at roundabout.

3.2. Priority and traffic light rules at roundabouts

The traffic management inside of the roundabout is based on a set of real-world driving patterns. In this paper, to control turning decisions and priority rules at the roundabout, we proposed a single-lane CA roundabout model based on a real-world roundabout model (see Fig. 2). This model allows drivers to make decision based on preferred driving directions according to their assigned trajectory (resp. shortest path) defined as a set of turning movements. Accordingly, to avoid conflict between entering and circulating vehicles inside the roundabout, the roundabout is operated based on the offside priority rule, which implies that a vehicle approaching a roundabout (on the entry leg) is usually required to give the right of way to circulating traffic inside the roundabout. Moreover, based on priority rules, the entering vehicles that request a right turning direction are allowed to access the roundabout without entering the roundabout circulatory roadway. However, circulating traffic has a priority at exit legs, which means that right-turning vehicles should stop to let circulating traffic exit the roundabout (see Fig. 3). On the other hand, when traffic lights are used instead of priority rules, the same rules still be adopted, but at each time period T_d, the traffic lights are switched to red or green color, and therefore only two entry lanes are enabled (horizontal or vertical lanes) (see Fig. 5).

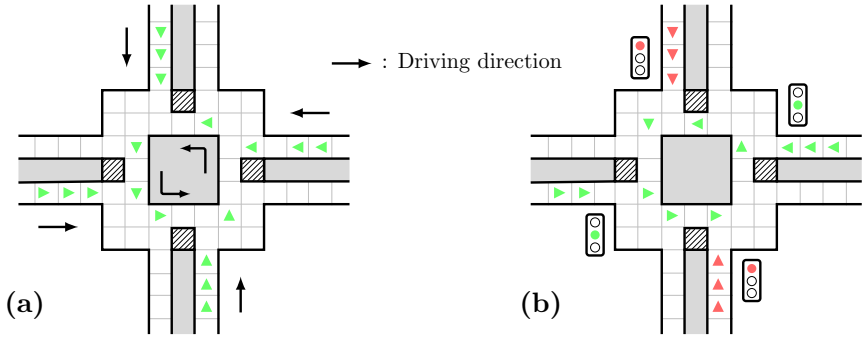

Fig. 5. Illustration of the proposed roundabout model with priority rules and with traffic lights.

Thereafter, we define the set of gaps used to control entering vehicles under the presence and absence of circulating traffic (see Fig. 3). Accordingly, we assume that a vehicle V_A tries to access the roundabout based on the offside priority rule. The gap $gap^1_A(t)$ (resp. $gap^1_B(t)$) represents the number of empty cells in front of the vehicle V_A (resp. V_B) at time t. For example in Fig. 3a, if the vehicle V_A turns right then $gap^1_A = gap'_a$ else $gap^1_A = gap_a$. Similarly, in Fig. 3b, if the vehicle V_B turn left then $gap^1_B = gap_b$ else $gap^1_B = gap'_b$. The gap $gap^2_A(t)$ (resp. $gap^2_B(t)$) represents the number of empty cells in front of the vehicle V_A (resp. V_B) and the collision cell at time t. Remember that there are two different cells where a conflict may occur; the first is at the entry leg while the second is on the exit leg of the roundabout. In the situation where a conflict occurred at the entry leg (see Fig. 3c), we have $gap^2_A = gap_c$ and $gap^2_B = gap'_c$. However, at

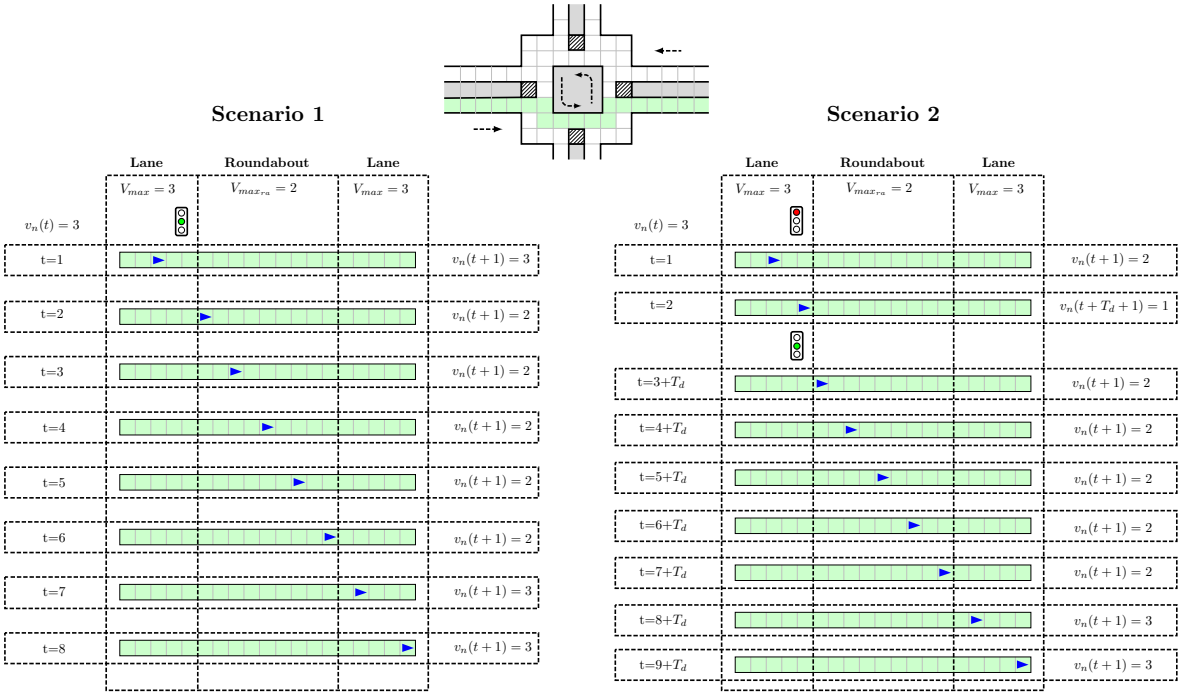

Fig. 6. Illustration example of two driving scenarios with the use of traffic lights, where T_d is the traffic light duration.

Algorithm 1 : Offside priority rule

1: **if** $(v_A(t) >= gap_A^2(t))$ **then**
2: **if** $(gap_B^2(t) >= v_{max_{rp}})$ **then**
3: $v_A(t+1) = min(v_A(t)+1, gap_A^1(t), v_{max_{rp}})$
4: $v_B(t+1) = min(v_B(t)+1, v_{max_{rp}})$
5: **else**
6: $v_A(t+1) = gap_A^2(t)$
7: $v_B(t+1) = min(v_B(t)+1, gap_B^1(t), v_{max_{rp}})$
8: **end if**
9: **end if**

the exit leg (see Fig. 3d), we have $gap_A^2 = gap_d$ and $gap_B^2 = gap'_d$. The offside priority rule is implemented via the algorithm (Algorithm 11). So, if the speed of V_A is higher or equal to gap_A^2 then the algorithm must be executed (line 1). The condition in line 2 means that when V_B is far away from the cell of collision, V_A enters safely into the roundabout. If not, V_A will move to just behind the cell of collision (line 6) (see Fig. 7).

In this context, we also define a Synchronized Traffic Light Control to alternatively give priority to waiting vehicles in the entry of roundabouts. Each entry lane is equipped with traffic lights which are governed by a cyclic duration TL_c. For each time period of length ($2\times T_d$) s, the traffic lights cycle is re-initialized. This implies that traffic lights are switched alternatively between green and red at each time interval T_d. When the traffic light is green, vehicles in the entry legs can enter the roundabout, whereas other vehicles should wait until the traffic lights are switched to green after a time interval T_d (see Algorithm 22).

3.3. Path planning strategy

In this part, we describe the proposed path planning strategy to allow each vehicle to request a shortest path during its travel toward a predefined destination. This strategy is based on the Bellman-Ford's shortest

Algorithm 2 : Traffic lights rule for roundabout

if (Traffic light is green **and** $v_A(t) >= gap_A^2(t)$) **then**
  if $(gap_B^2(t) >= v_{max_{rp}})$ **then**
    $v_A(t+1) = min(v_A(t)+1, gap_A^1(t), v_{max_{rp}})$
    $v_B(t+1) = min(v_B(t)+1, v_{max_{rp}})$
  else
    $v_A(t+1) = gap_A^2(t)$
    $v_B(t+1) = min(v_B(t)+1, gap_B^1(t), v_{max_{rp}})$
  end if
else
  $v_A(t+1) = gap_A^2(t)$
  $v_B(t+1) = min(v_B(t)+1, gap_B^1(t), v_{max_{rp}})$
end if

path algorithm [38] due to its high standing as it is widely used to solve several problems including network routing and optimal route planning in navigation systems.

In this paper, vehicles can request shortest paths based on the proposed path planning strategy by processing the Bellman-Ford algorithm. We consider the travel time instead of the distance between each pair of edges according to the traffic network-based graph. Using the following algorithm and based on measurement of the travel time in each road segment as an indicator of the current traffic state in that road segment. At each time period, the travel time in each road segment is calculated based on the combination of two known equations. The first equation Eq. 1 is introduced in NaSch model to estimate the traffic flow based on the correlation between density, speed, and traffic flow. The second equation Eq. 2 represents the hydrodynamic relationship between density, speed and traffic flow [6, 39].

$$\mathbf{J}(\rho) = \begin{cases} \rho(v_{max} - p), & \text{if } \rho <= \rho_c, \\ \\ (1-p_0)(1-\rho), & \text{if } \rho > \rho_c. \end{cases} \tag{1}$$

$$\mathbf{J}(\rho) = \rho v \tag{2}$$

where $\rho = \dfrac{D_{ij}}{N}$ is the density of vehicles and D_{ij} is the length of road segment between two successive intersections i and j.

Based on the correlations between time, distance, and speed ($T = \frac{D_{ij}}{v}$), we find that the travel time is given by:

$$T_t(\rho) = \begin{cases} \dfrac{D_{ij}}{\dfrac{\rho(v_{max} - p)}{\rho}}, & \text{if } \rho <= \rho_c, \\ \\ \dfrac{D_{ij}}{\dfrac{(1-p_0)(1-\rho)}{\rho}}, & \text{if } \rho > \rho_c. \end{cases} \tag{3}$$

According to the equation Eq. 4 the shortest path could be generated by taking into account the traffic state in terms of travel time. The state of the traffic network-based graph is updated periodically. Thus, at every time step, by applying the Bellman–Ford algorithm each vehicle can request the shortest path under a changing traffic state versus time. The Bellman–Ford equation is given as follows:

$$T_t(i,j) = \min_{k \in Intersections\ set} \{T_t(i,k) + T_t(k,j)\} \tag{4}$$

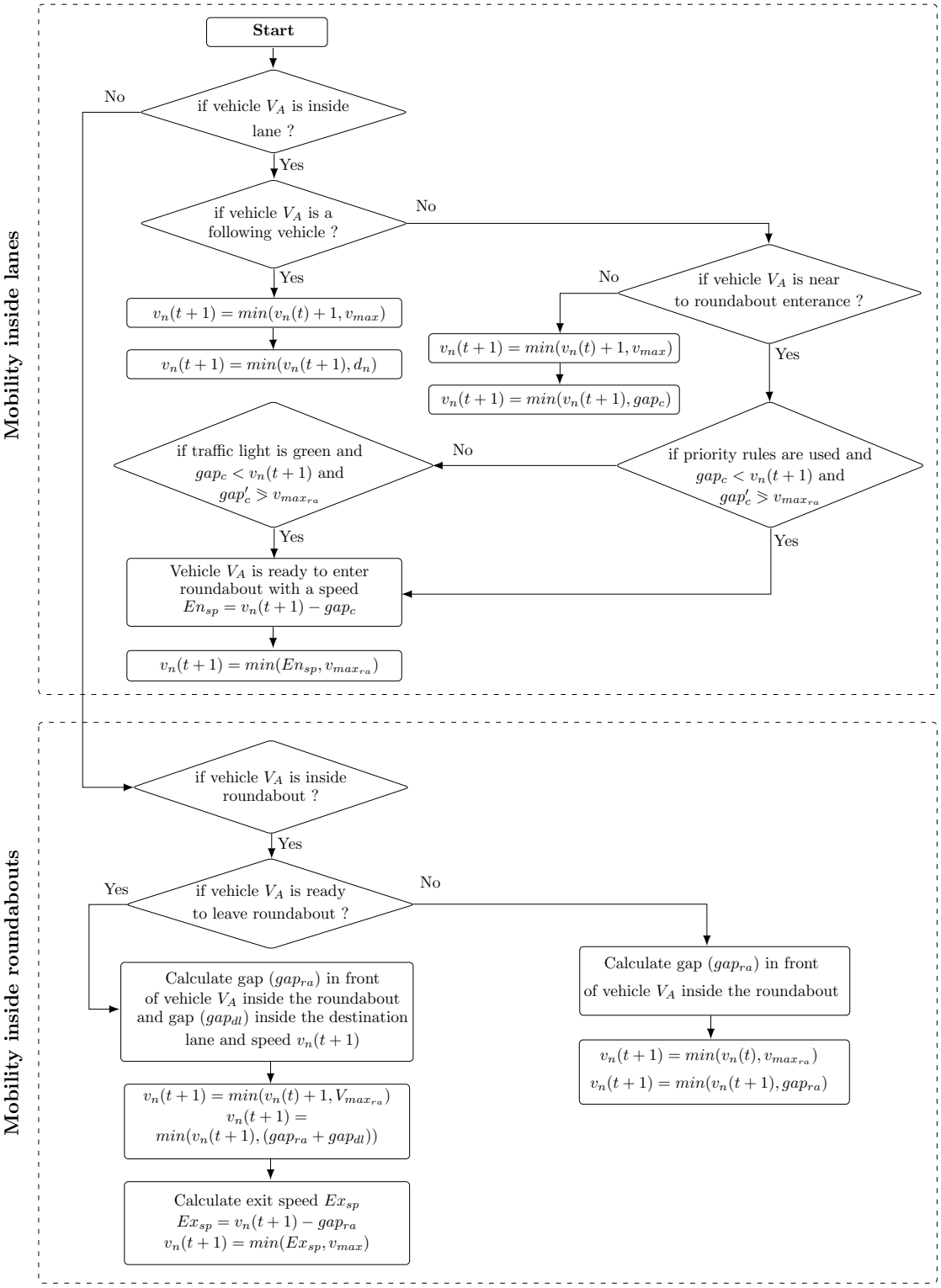

Fig. 7. Flowchart of the proposed mobility rules at roundabouts and road segments.

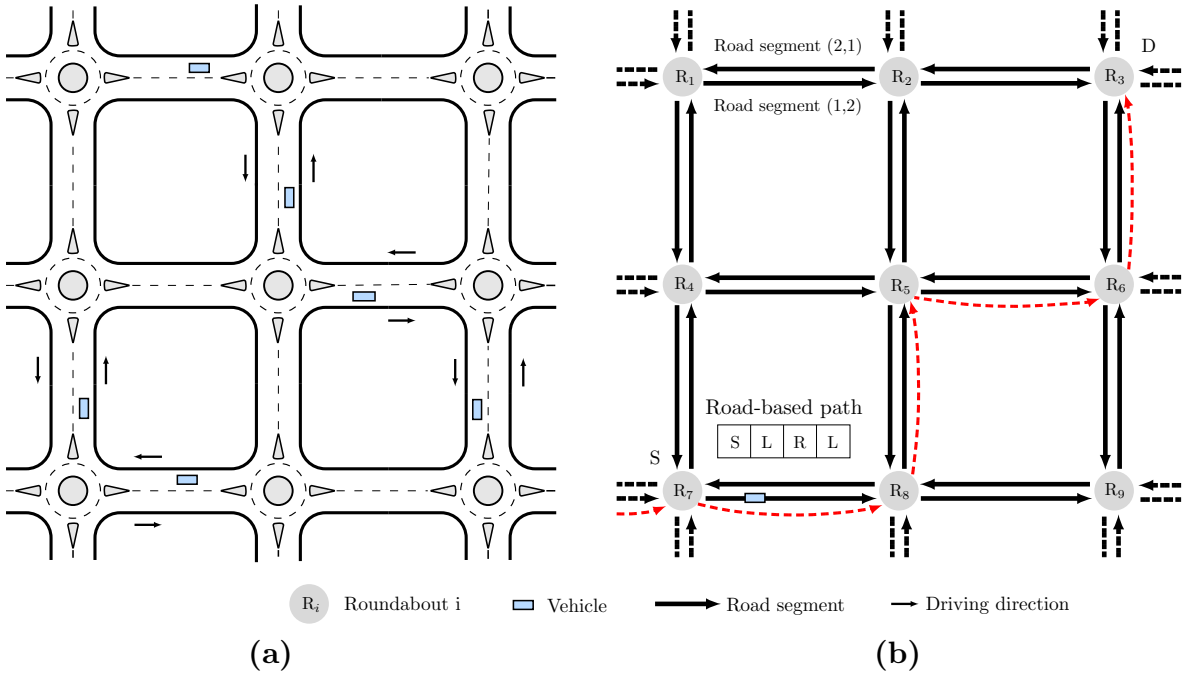

Fig. 8. Illustration example of path planing based on Bellman-ford algorithm.

where $T_t(i,k)$ (resp. $T_t(k,j)$) represents the travel time for road segment $Roid_s(i,k)$ (resp. $Road_s(k,j)$) between two successive intersections (i, k) (resp. k, j). Indeed, each shortest path calculated with the Bellman–Ford algorithm is transformed further into a sequence of turning movements (i.e., left turn, right turn, u-turn, or straight ahead) which allows a vehicle easily make a decision corresponding to their predefined destinations when they reach a such roundabout.

Based on the proposed path planning strategy that takes into account the traffic state in terms of travel time in each road segment, it is expected that the travel time would be decreased significantly as vehicles are able to avoid such congested regions and select the best trajectories.

4. Connectivity and network performance analysis

4.1. Mobility scenario

We simulated traffic scenarios based on a Manhattan two-dimensional network of 2000 × 2000 m^2, where 100 roundabouts are deployed at the intersections of vertical and horizontal streets (i.e., 10 roundabouts at each lane). The distance between roundabouts is determined at the beginning of the simulation (K=20 cells). At the beginning of the simulation, vehicles are assigned random origin-destination pairs to allow vehicles travel from origins to predefined destinations.

To include intelligent aspects of mobility for drivers, vehicles are assigned shortest paths based on a centralized path planning strategy to provide re-routing of vehicles during their travel. The computation of assigned shortest paths is done based on the Bellman–Ford algorithm and the collected information in terms of travel time at road segments. Afterwards, the shotest paths are converted to a set of turning movements (i.e., right, left, straight ...) to allow a such vehicle determine if it will continue moving in the straight direction or it will make turn to a specific direction when reaching a roundabout (i.e., right, left, or U-turn). Moreover, the path planning strategy allows a periodic update of vehicles trajectories in terms of the current traffic state.

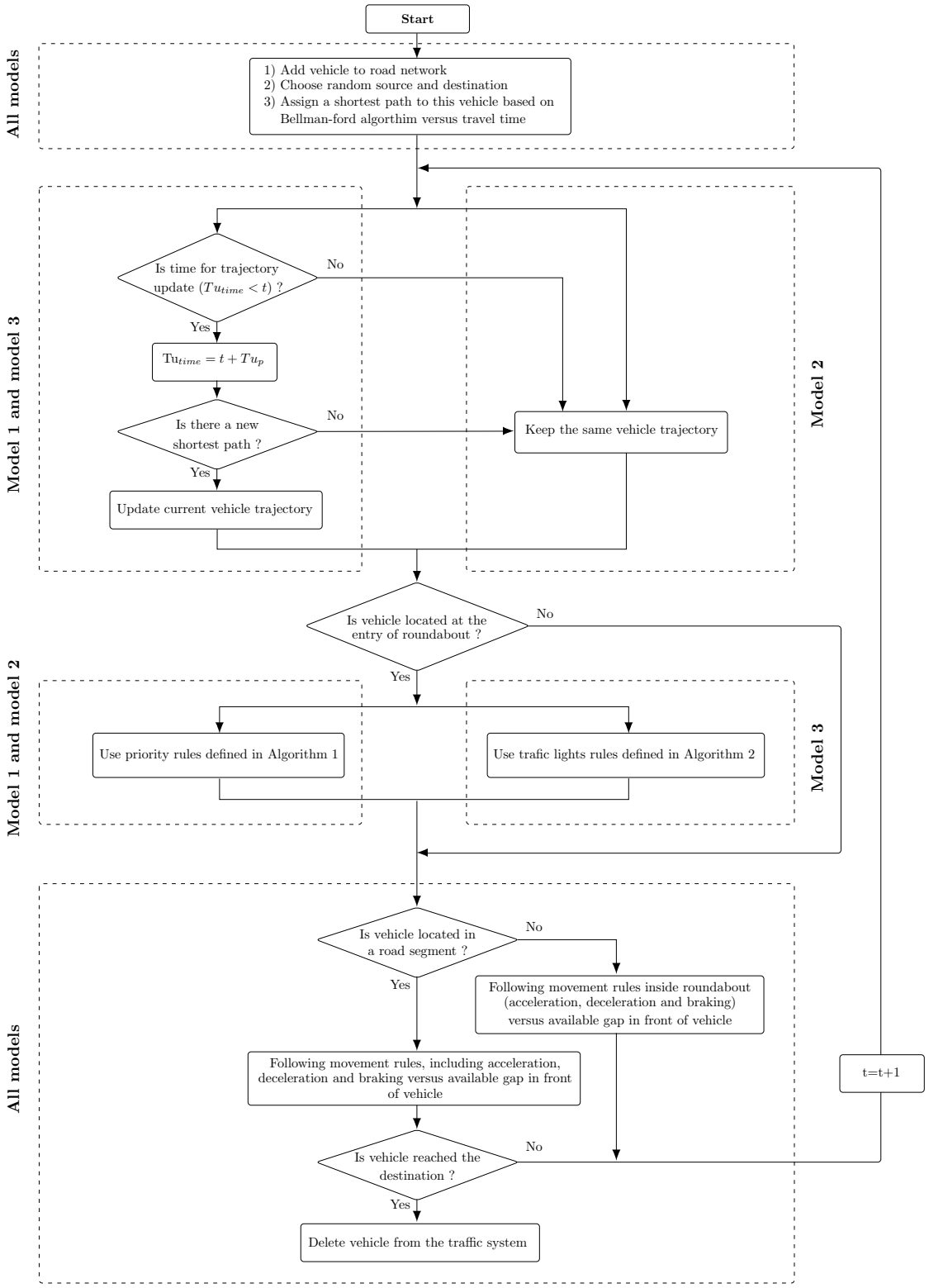

Fig. 9. Illustration of life cycle of a vehicle in the traffic system.

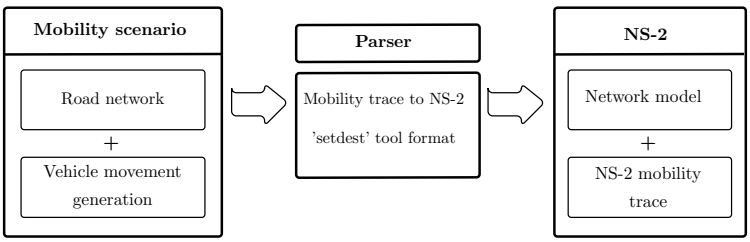

Fig. 10. Framework for generating .tcl file of the proposed traffic scenario to be used in network simulator NS-2.

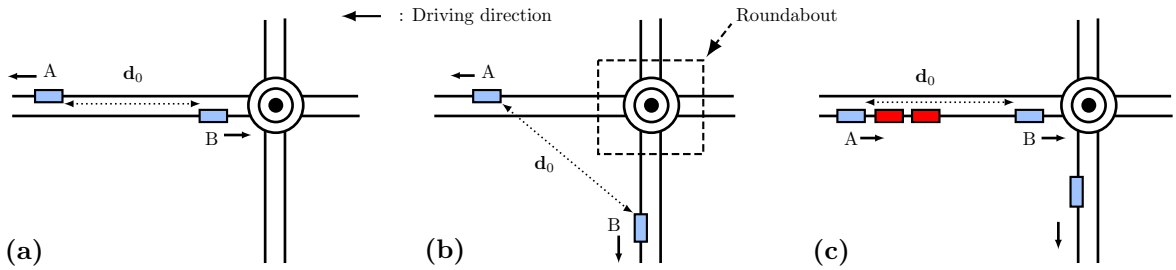

Fig. 11. Illustration of different link failures causes considered in our investigation.

To keep a specific vehicle density into the road network, we inject a fixed number of vehicles at the beginning of the simulation. Thus, when a vehicle reaches its destination, that vehicle will be removed and replaced by a new one with different origin–destination pair (see Fig. 9).

Based to the above assumptions, three mobility designs are introduced:

- The first mobility model is denoted by (BA-Realtime) and it allows vehicles to follow priority rules at the roundabout while performing real-time re-routing of their trajectories periodically based on the proposed path planning strategy.
- The second mobility model is denoted by (BA-Fullroad) and it is similar to the first one, but vehicles do have not the ability to update their trajectories when they reach a roundabout.
- The third model is denoted by (BA-Realtime+TL) and it extends the first model while traffic lights at roundabouts are used instead of priority rules (see Fig. 6).

At each time step, mobility traces are generated by providing extra mobility information such as vehicle direction, which will be useful when analyzing wireless link break causes (see Fig. 10). At the end of the simulation, the mobility traces are converted to NS-2 .tcl format. Accordingly, some modifications on NS-2 have been realized to take into account vehicles' mobility directions in the output traces of NS-2, which will help in the statistical part as we need to make measurements of link break causes after the simulation end.

4.2. The network model

We consider a vehicular network consisting of (N>0) nodes (vehicles), where each node can generate packets periodically with a generation rate of (2.5 packet/s). In addition, A finite queue of size S is associated with each node.

In this model, we define 10 connections (i.e. 10 sources and 10 destinations) where other nodes are considered as relay nodes. Each source node/vehicle i attempts to send periodically UDP packets to a predefine destination node/vehicle. On the other hand, when a node/vehicle reaches its destination of travel, this vehicle will be removed and replaced by another one with a random location (see Fig. 9), but the associated node i with the deleted vehicle will be reassociated with the new injected vehicle. A two-ray ground propagation model is used while the IEEE 802.11p protocol is used at the MAC layer. The exchange

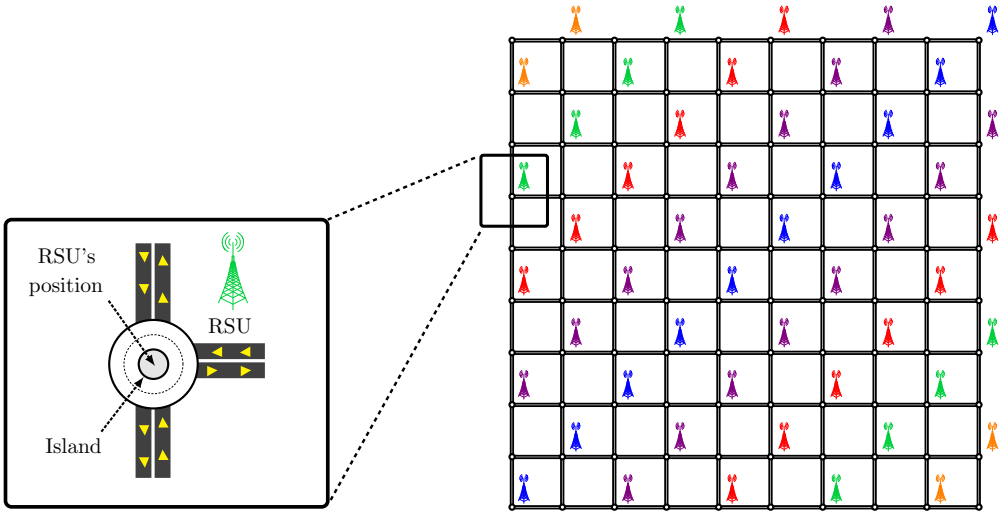

Fig. 12. RSUs positions in the network area. The four simulated cases are distinguished by colors: 10-RSUs displayed as blue units; 30-RSUs: blue+red+green; 40-RSUs: blue+violet+red+$\frac{1}{2}$(orange); 50-RSUs: blue+violet+red+green+orange.

Table 2. Simulation parameters for mobility models.

Parameter	Symbol	Value
Roadmap size	L× L	2 km× 2 km
Number of vehicles	N	20-7200
Maximum speed for vehicles outside the roundabout	v_{max}	3 (cells/second)
Maximum speed for vehicles inside the roundabout	$v_{max_{ra}}$	2 (cells/second)
Number of roundabouts on each two-way street	N_{ra}	10
Distance between roundabouts	K	20 (cells)
The length of a single cell [40]	C_{len}	7.5 m
The number of detector sites	N_d	36
Time step increment	dt	1 s
Traffic light duration	T_d	{30 s and 60 s}
Time period to update vehicle trajectory	Tu_p	5 s
Traffic light cycle	TL_c	2×T_d

of communications is provided via a multi-hop routing where vehicles collaboratively send and relay traffic according to AODV routing protocol. The simulation parameters used for the network model are depicted in 2.

4.3. Indicators of system performance

In this section, based on several performance metrics, we monitor the impact of different effective factors, including those related to the transportation system and those related to network behavior. Accordingly, all proposed performance metrics considered in this work are described in detail as follows:

- **Average speed:** we define the average speed as of average of vehicles' speeds during overall simulation time interval, where for one time step, it can be calculated as :

$$\textbf{Average speed} = \frac{1}{N}\sum_{i=1}^{i=N} v_i(t) \tag{5}$$

Table 3. Simulation parameters for network model.

Parameter	Value	Parameter	Value
Simulation area	2 km × 2 km	Symbol duration	8 μs
Version of the simulator	NS-2.35	Frequency	5.9 GHz
Simulation time	500 s	SIFS	32 μs
Propagation model	TwoRayGround	TDFS	58 μs
IEEE standard	802.11p	CW minimum size	15
Bandwidth	10 Mbps	CW maximum size	1023
Interface queue model	PriQueue	CW slot time	13 μs
Routing Protocol	AODV	Queue size	64 packets
Transport protocol	UDP	Packet size	1 KB
Packet generator	CBR	Packet generator interval	2.5 packet per second
Transmission range	R={250 m, 150 m and 80 m}	Transmission range of RSUs	150 m

- **Traffic flow:** we define the traffic flow $J_{det_{(i)}}$ as the number of vehicles crossing a detector site i per unit time. We use many detectors ($\mathbf{N}_d$) placed at different positions in the road network. The traffic flow is defined as follows:

$$\textbf{Traffic flow} = \frac{1}{N_d} \sum_{i=1}^{i=N_d} J_{det_{(i)}} \tag{6}$$

- **Average travel time:** we define the travel time as a sequence of time intervals that characterize the resulting time interval between injection time ($t^{(i)}_{inject}$) when the vehicle starts moving from a source location and the arrival time ($t^{(i)}_{arriv}$) when the vehicle reaches the destination location where M is the total number of vehicles that reached their destinations before the end of simulation. The travel time is defined as follows:

$$\textbf{Average travel time} = \frac{\sum_{i=1}^{i=M}(t^{(i)}_{arriv} - t^{(i)}_{inject})}{M} \tag{7}$$

- **Average end-to-end delay:** we define the end-to-end delay as a sequence of time intervals that characterizes the resulting time period including the data transmission delay, the propagation delay, the nodal processing delay, and the queuing delay at each intermediate node. We then calculate the end-to-end delay as the difference between the send time ($t^{(i)}_{sen}$) and the received time ($t^{(i)}_{rec}$) of the successfully received packet by the destination, where $nbr_{(packs)}$ is the total number of received packets. The average end-to-end delay is defined as follows:

$$\textbf{EED} = \frac{\sum_{i=1}^{i=nbr_{(pack)}}(t^{(i)}_{rec} - t^{(i)}_{sen})}{nbr_{(packs)}} \tag{8}$$

- **Packet delivery ratio:** we define the packet delivery ratio as the total number of packets successfully received by the destination (rec_{packs}) over the communication channel divided by the total number of data packets sent from the source nodes (sen_{packs}).

$$\textbf{PDR} = \frac{rec_{packs}}{sen_{packs}} \tag{9}$$

- **Link duration:** we define the link duration delay as a sequence of time intervals that characterizes a valid link between a pair of nodes. We then calculate the link duration as the difference between the setup time of a wireless link between two nodes ($t^{(i)}_{set}$) and the time of wireless link failure ($t^{(i)}_{fail}$), where

nbr_{links} is the total number of the established wireless links. The average link duration is defined as follows:

$$\mathbf{LD} = \frac{\sum_{i=1}^{i=nbr_{links}} (t_{fail}^{(i)} - t_{set}^{(i)})}{nbr_{links}} \tag{10}$$

5. Simulation results and discussions

In this section, first, we need to validate the feasibility and the effectiveness of our path planning strategy, and therefore show how each mobility design can affect the traffic system. To that end, a set of performance metrics, including traffic flow, average speed and travel time are introduced to show a detailed picture of the system performance from different sides. The validation and analysis of mobility designs are done under varying vehicle densities and maximum speeds.

In the second part, the network performance and connectivity dynamics are analyzed according to different mobility designs and other varying effective factors. Thus, the overall set of effective factors considered in this work is described as follows:

- Vehicle mobility model, including three different mobility models: BA-Realtime, BA-Fullroad, and BA-Realtime+TL with two different traffic lights' durations ($T_d = 30$ s and 60 s).
- The effect of transmission range, where the transmission range varies in $\{250\text{ m}, 150\text{ m}, 80m\}$, while the mobility model is fixed to BA-Realtime.
- The effect of RSUs deployment strategy, including RSUs' number that varies in $\{10, 30, 40, 50\}$ and RSUs' positions (i.e. the way the RSUs are deployed in the network area), while the mobility model is fixed to BA-Realtime.
- Analysis of link failures in terms of link duration and the last cause of link break under two different maximum vehicles speed (v_{max}=81 km/h and 135 km/h), while the mobility model is fixed to BA-Realtime.

The simulation results are provided based on several performance metrics, including packet delivery ratio, paths length, link duration, and end-to-end delay. The simulation of network scenarios is performed by using the Network Simulator NS-2.35 with 60 runs. The parameters used in the simulation for both mobility and network model are summarized in 2 and 3.

5.1. The effect of mobility designs on traffic state

In this section, we aim to analyze and reveal the characteristics of the traffic system under varying parameters. First, the impact of three different mobility designs (BA-Realtime, BA-Fullroad and BA-Realtime+TL) on the traffic system is analyzed, while the maximum speed v_{max} is fixed to 81 km/h (3 cells) and the vehicle density is varied in [0,1] (see Fig. 13a and Fig. 13b). For BA-Realtime+TL mobility model, two different traffic light durations $T_d = 30$ s and 60 s are used, respectively. We adopt two main performance metrics for analysis, including average speed and traffic flow, respectively.

Second, we analyze the traffic system in terms of travel time distributions according to two different vehicles density ($\rho = 0.1$ and $\rho = 0.3$), while the maximum speed v_{max} is fixed to 81 km/h (see Fig. 13c and Fig. 13d).

As plotted in Fig. 13a, the traffic flow and average speed versus vehicles' density reproduces the free flow state observed in real traffic flow, where vehicles move relatively at high speed. By comparing these results, we can observe that both BA-Realtime and BA-Fullroad outperform BA-Realtime+TL (BA-Realtime model with traffic lights control). This is because traffic lights have a significant impact on the dynamics of vehicles. Furthermore, the traffic lights have also effects on travel time as observed from Fig. 13c.

Fig. 13a-b show that in the case of BA-Fullroad, the transportation system exhibits a gridlock state due to propagation of a traffic jam wave as a result of local deadlock at some nearby roundabouts [41]. This situation can occur mainly due to a perturbation between two types of traffic flow: circulating vehicles inside

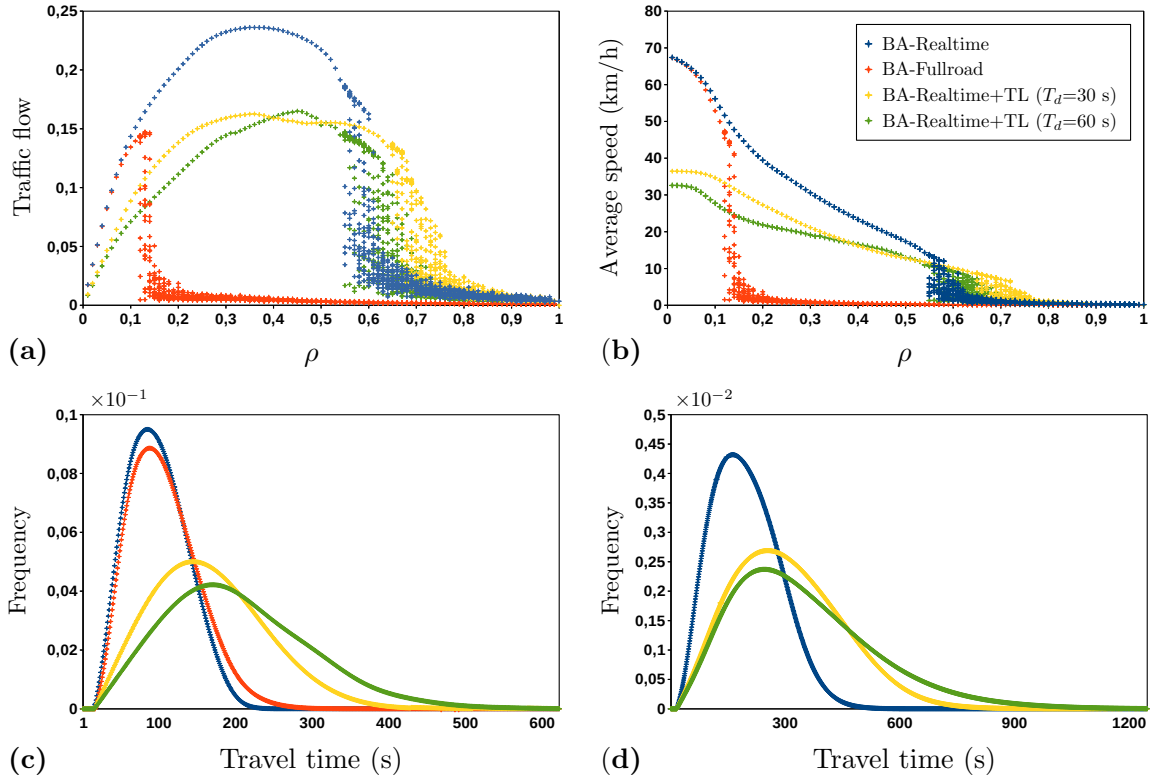

Fig. 13. Effect of increasing the network density N: (a) Traffic flow, (b) Average speed, (c) and (d) Average travel time under two different vehicle densities ($\rho = 0.1$ and $\rho = 0.3$). The maximum speed $v_{max} = 81$ km/h is equivalent to 3 (cells/s).

the roundabout and exiting vehicles. This phenomenon in turn is due to non-equilibrium in the turning movements balance, where a high number of vehicles choose the same turning direction. On the other hand, as BA-Fullroad mobility model allows vehicles to request unchangeable short paths versus time between the assigned origin and destination which allows vehicles to keep the same trajectory, and therefore this cannot help drivers in avoiding to pass through congested regions. Based on the comparison between BA-Fullroad and BA-Realtime, we can see that BA-Realtime is more efficient and exhibits the highest traffic flow rate because vehicles update continuously their trajectories which leads to the avoid congestion in road segments.

Under the congested state, we observe that BA-Realtime still always outperforms other mobility models by a large margin when comparing traffic flow, average speed, and travel time. Also, we can see that the traffic lights' duration (T_d) has a significant impact on the traffic state in the case of BA-Realtime+TL mobility model. When increasing the parameter T_d, both the traffic flow and average speed decrease, and, consequently, the travel time will increase. This may happen because of the increase in the waiting time resulted before the traffic lights are switched to green. In this case, a considerable proportion of vehicles slow down and make a stop, and therefore this absolutely will have an effect on the travel time.

Under high vehicles' density ($\rho > 0.5$), we can observe an appearance of an unexpected gridlock state for all mobility models. But, we also notice that in the case of BA-Realtime and BA-Realtime+TL (T_d = 60 s), the traffic state transition to gridlock occurs early (at $\rho \simeq 0.55$) than other mobility models such as BA-Realtime+TL (T_d = 30 s), whereas for BA-Realtime+TL (T_d = 30 s), the gridlock appears until ($\rho \simeq 0.65$). This can be explained by the fact that both BA-Realtime and BA-Realtime+TL (T_d = 60 s) fail to handle the equilibrium between traffic dynamics and the rapid increase in vehicle density. Regardless that real-time planning of traffic can allow vehicles to choose the best paths, sometimes a higher number of vehicles may request the same road segments at the same time period as these ones provide less travel time. This can result in the appearance of congested or saturated lanes because they are part of a higher

number of trajectories. But, in the case of BA-Realtime+TL (T_d=30 s), we can say that the reason for delayed gridlock is related to the fact that the used traffic lights duration allows an equilibrium in the traffic dynamics as it helps in avoiding queueing in road segments.

Fig. 13c and Fig. 13s show that the travel time could be improved significantly when real-time planning of vehicles' trajectories is provided. This is, for example, the case of BA-Realtime and BA-Fullroad models regardless that BA-Fullroad does not allow a periodic update of vehicles' trajectories versus time. Accordingly, we observe that BA-Realtime outperforms BA-Fullroad by a significant margin due to its ability to update vehicles' trajectories as a function of traffic state (see Fig. 13c). However, both BA-Realtime and BA-Fullroad models dramatically outperform BA-Realtime+TL mobility model because vehicles are forced to stop at intersections when the traffic light is switched to red, which increases the travel time by an extra amount of time. Also, as we can see in Fig. 13d, both the increase in vehicles' density and traffic lights duration (T_d) have a significant impact on travel time. The increase in vehicles' density leads to a rapid decrease in the travel time due to a strong relationship between vehicles' moving speed and vehicles density.

5.2. The effect of transmission range

In this section, we analyze the impact of mobility models under varying transmission range on both the network performance and connectivity condition while increasing the network density. At that end, the maximum speed is fixed to 81 km/h (3 cells), while the transmission range varies into $\{250\text{ m}, 150\text{ m}, 80\text{m}\}$. We used two different traffic light durations (T_d = 30 s and 60 s) in the case of the mobility model with traffic lights (BA-Realtime+TL).

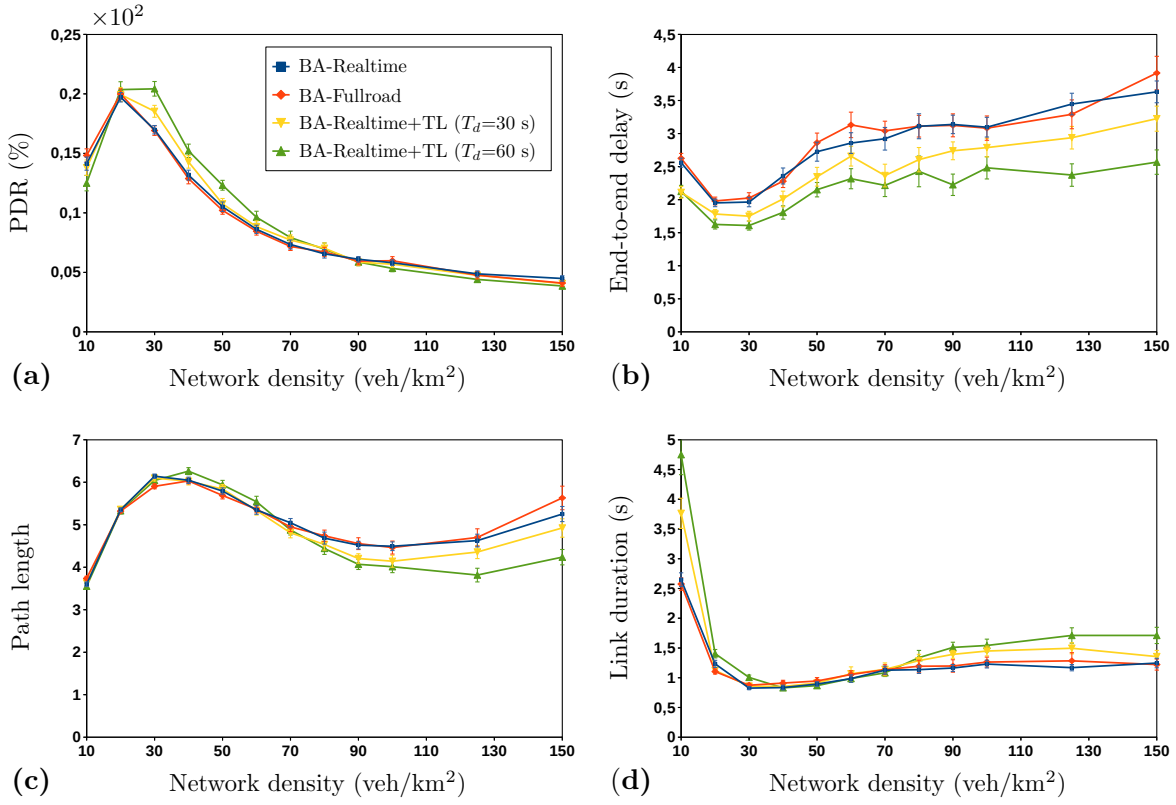

Fig. 14. Effect of increasing the network density and varying the vehicle mobility with parameters R = 250 m: (a) Packet delivery ratio, (b) End-to-end delay, (c) Path length, and (d) Link duration. The maximum speed v_{max} = 81 km/h and the number of RSUs is 10.

First, we analyze the network reliability according to several performance metrics, including packet

delivery ratio, paths length, link duration, and end-to-end delay (see Fig. 14, Fig. 15 and Fig. 16). Second, we analyze the network reliability and connectivity condition based on the distributions of packet delivery ratio, end-to-end delay, link duration, and path length, while the network density N is fixed to 40 $vehs/km^2$ (see Fig. 17), firstly, and then, is fixed to 320 $vehs/km^2$ (see Fig. 18).

Fig. 14 shows that mobility models with traffic lights outperform the other mobility models when comparing the obtained results in terms of packet delivery ratio, end-to-end delay, and link duration. We can explain that by the fact that the traffic lights play a positive role in allowing vehicles to stay connected for a long time. Also, we observe that the network performance increases as the traffic lights duration (T_d) increases. However, when the number of vehicles becomes higher (N>= 90 $vehs/km^2$), we observe that the packet delivery ratio is the same regardless of the mobility model. Fig. 14c–d shows that under high network density, both BA-Realtime and BA-Fullroad models cause an increase in both the path length and end-to-end delay, whereas a decrease in the link duration is observed. But, in the case of BA-Realtime+TL mobility model, both the link duration and end-to-end delay could be improved and a decrease in the path length is observed. We can conclude that both the increase in network density and traffic lights duration have an impact on the connectivity condition of the network by helping in establishing short paths between vehicles.

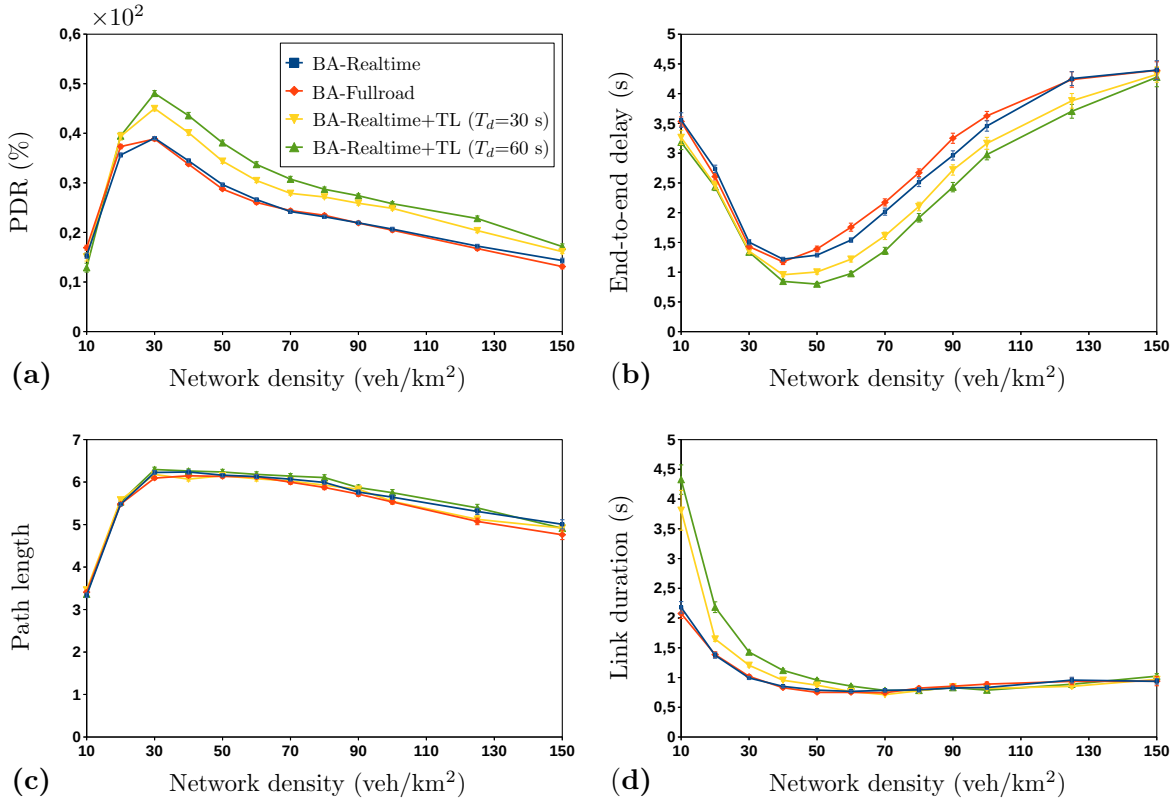

Fig. 15. Effect of increasing the network density and varying the vehicle mobility with parameters R = 150 m: (a) Packet delivery ratio, (b) End-to-end delay, (c) Path length, and (d) Link duration. The maximum speed v_{max} = 81 km/h and the number of RSUs is 10 (color blue).

As shown in Fig. 15, by decreasing the transmission range to (R = 150 m), we can observe that the network performance is improved as compared with the obtained results in the case of a higher transmission range (R = 250 m) regardless of vehicle mobility model. This can be explained by the fact that the increase in the transmission range, may lead to an increase in the number of interferer senders, therefore, this may degrade the overall network performance. On the contrary, a decrease in transmission range improves the

accessibility to network but may have a negative impact on the connectivity condition when the network density is very low. On the other hand, BA-Realtime+TL mobility model depicts an improvement in terms of packet delivery ratio, end-to-end delay, and link duration, especially under low network density. This means that this model fits well with the low network density when compared with both BA-Realtime and BA-Fullroad mobility models. However, Fig. 15c and Fig. 15d show that the path length and link duration remain almost the same regardless of the mobility model, especially under low network density. Then, we can conclude that the difference lies in the fact that the waiting time before traffic lights are switched to green allows vehicles to form in some way a stable network' topology which provides a supplementary profit in terms of network connectivity.

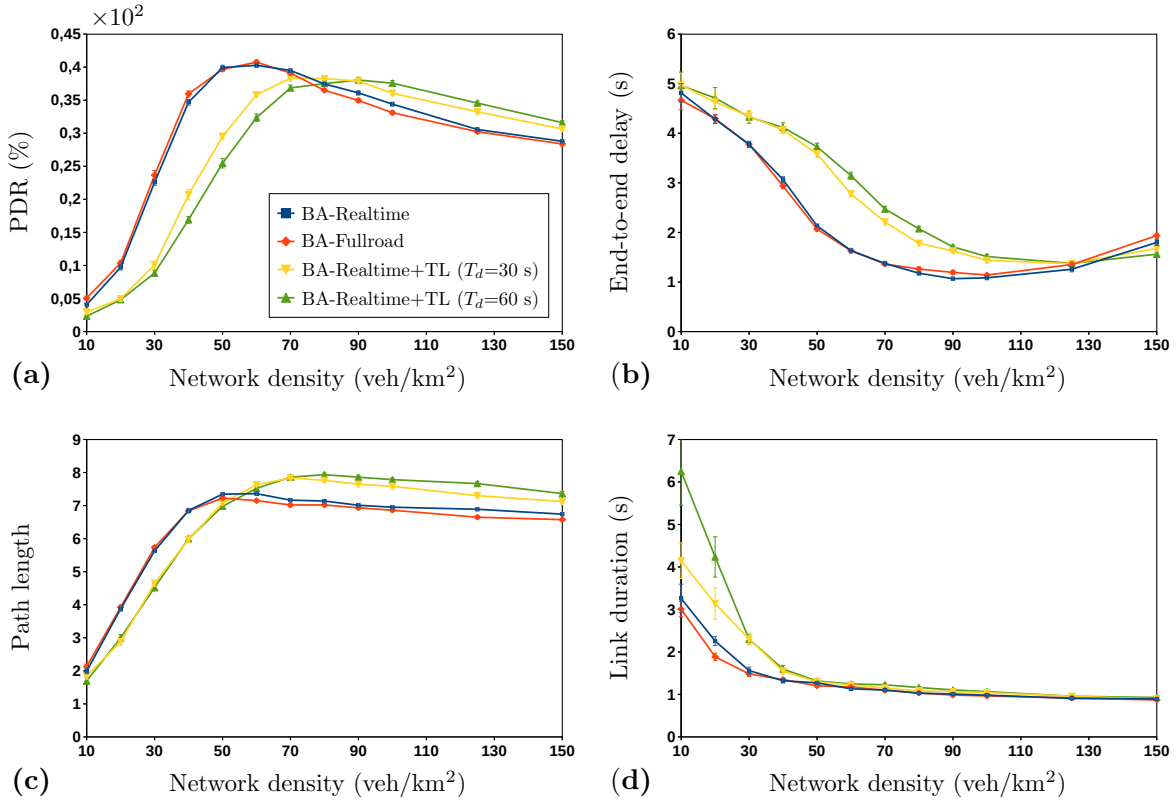

Fig. 16. Effect of increasing the network density and varying the vehicle mobility with parameters R = 80 m: (a) Packet delivery ratio, (b) End-to-end delay, (c) Path length, and (d) Link duration. The maximum speed v_{max} = 81 km/h and the number of RSUs is 10 (color blue).

Fig. 16 shows the network performance under a decreased transmission range (R = 80 m). As we can see, under low network density (N<= 40 $vehs/km^2$), the network performance is significantly decreased as compared to previous results with (R = 250 m and 150 m). This can be explained by the fact that the network connectivity is significantly affected by the decrease in the transmission range, where vehicles might move out of the transmission range more quickly, and therefore the wireless links between vehicles may fail. Thus, under these conditions, such an established wireless link between two vehicles may remain active only for a relatively short time before a sudden break occurs. This may lead to high packets loss due to a difficulty to establish a connection between the source and destination as a result of the increased probability of link break and saturated queue of source node due to unavailable path. The results in terms of path length confirm that only paths with a small length are allowed to be established between vehicles, while long ones are susceptible to frequent link breaks. We also observe that the network exhibits two main phases in the case of (N<70 $vehs/km^2$) and (N> 70 $vehs/km^2$), where under low network density, Fig. 16 depicts a continuous

improvement of network performance (Phase 1), whereas, in the case of sufficiently higher network density (Phase 2), the network performance starts to decrease, but slightly. In the first phase, the mobility models without traffic lights outperform that with traffic lights for the first time. We can explain that by the fact that under low network density and the presence of traffic lights, vehicles are forced to follow a trajectory consisting of a sequence of stops (when traffic lights are switched to red). This is expected to cause some crowded vehicles at crossings and an unexpected split of vehicles clusters into two sub-clusters of vehicles, where vehicles in the first one will slow down and make a stop at the crossing, and vehicles in the second one will continue moving. This situation will have a significant impact on wireless links' lifetime, especially under free flow and short transmission range because both these parameters may quickly contribute to an occurrence of link failure. But, under increased network density (Phase 2), the established paths will be more stable due to a decrease in the vehicles' speed, and therefore the connectivity gets improved again. Regardless that the increase in vehicle density helps in improving the connectivity, especially in the case of traffic lights; however, a higher rate of link failures will also result due to unexpected vehicles stop at roundabouts when the traffic lights are switched to red. The increase in the link failures in turn is expected to lead to a high number of attempts by vehicles to re-establish connections with their destinations at the same time. This would lead to an increased probability of collisions between sending nodes during the contention-based random access phase provided by the IEEE 802.11p protocol, and therefore this delays the association of vehicles (source nodes) to their destination nodes, which results in an increased end-to-end delay (see Fig. 16b). However, the network performance under a low transmission range seems to be more accommodating for the considered mobility scenario as compared with previous values of transmission range.

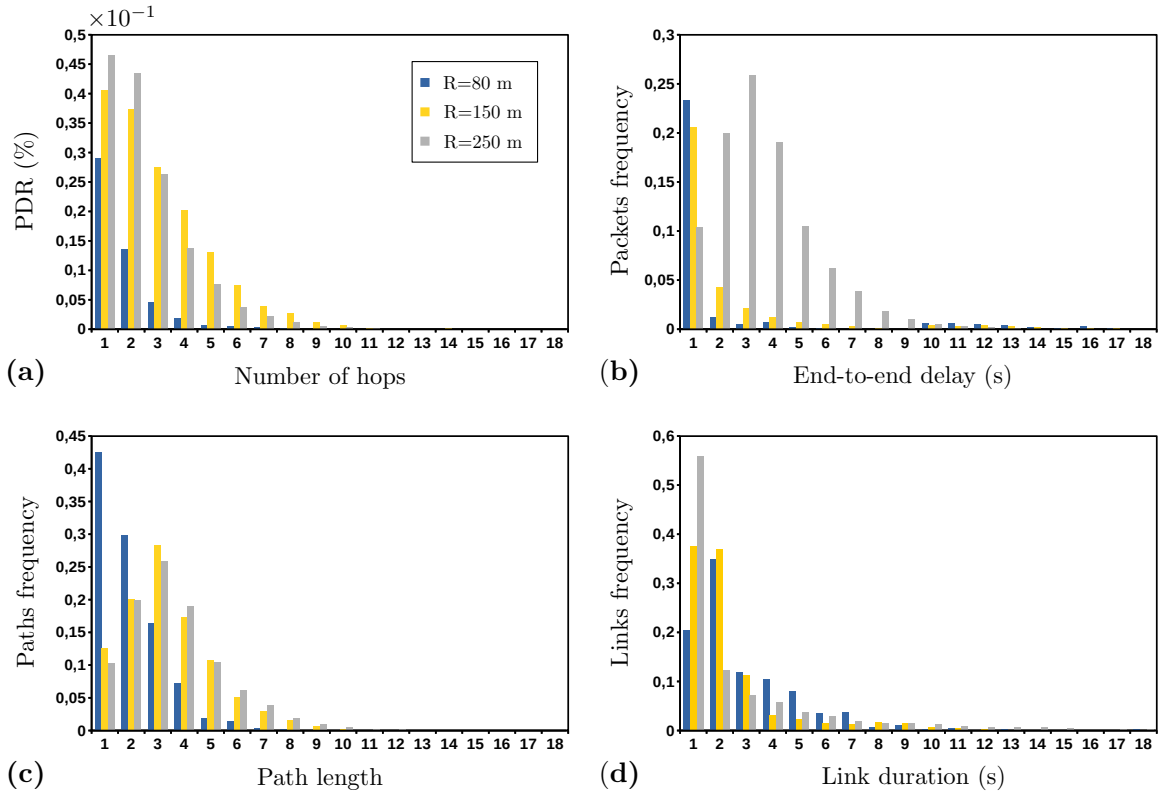

Fig. 17. Distribution of Packet delivery ratio (a), End-to-end delay (b), Path length (c), and Link duration (d) with low network density and varying transmission radius (R = 250 m, R = 150 m, and R = 80 m). The used mobility model is BA-Realtime, network density is 40 $vehs/km^2$, maximum speed v_{max} = 81 km/h and the number of RSUs is 10 (color blue).

Fig. 17 and Fig. 18 show a comparison in terms of distributions of packet delivery ratio, average end-to-

end delay, path length and link duration under different transmission ranges (i.e., R = 80 m, R = 150 m and R = 250 m) for two different network densities (40 $vehs/km^2$ and 320 $vehs/km^2$). As illustrated in Fig. 17a, the packet delivery ratio as a function of the number of hops under low network density increases while increasing the transmission range. Moreover, we notice that the increase in the packet delivery ratio is due to an increase in the ratio of the received packets at a higher number of hops. This means that under increased transmission range, the established paths are long enough to allow the source and destination vehicles to establish successfully a connection (see Fig. 17c). However, the results in Fig. 17b show clearly that under increased transmission range (R = 250 m), a higher number of packets are received with a low end-to-end delay due to a high level of connectivity. On the contrary, under a low transmission range, the end-to-end delay slightly increases, especially for long-established paths, due to frequent links break, and therefore, this may cause a routing overload when a routing process is launched to find a new path to replace the old one (i.e., this includes requests packets, Request-To-Send (RTS) and Clear-To-Send (CTS) control packets and errors packets which are related to the frequent route discovery process and link failures). On the other hand, the observed high frequency of paths with small lengths means that the sender vehicles can often establish short paths based on some neighbor vehicles when the destination is located in the neighborhood (i.e., this includes following vehicle, leading vehicle, and some RSUs). In the contrast, the inability to establish paths with the destination during certain intervals of time is expected to cause a higher data loss due to saturated queues at sender vehicles.

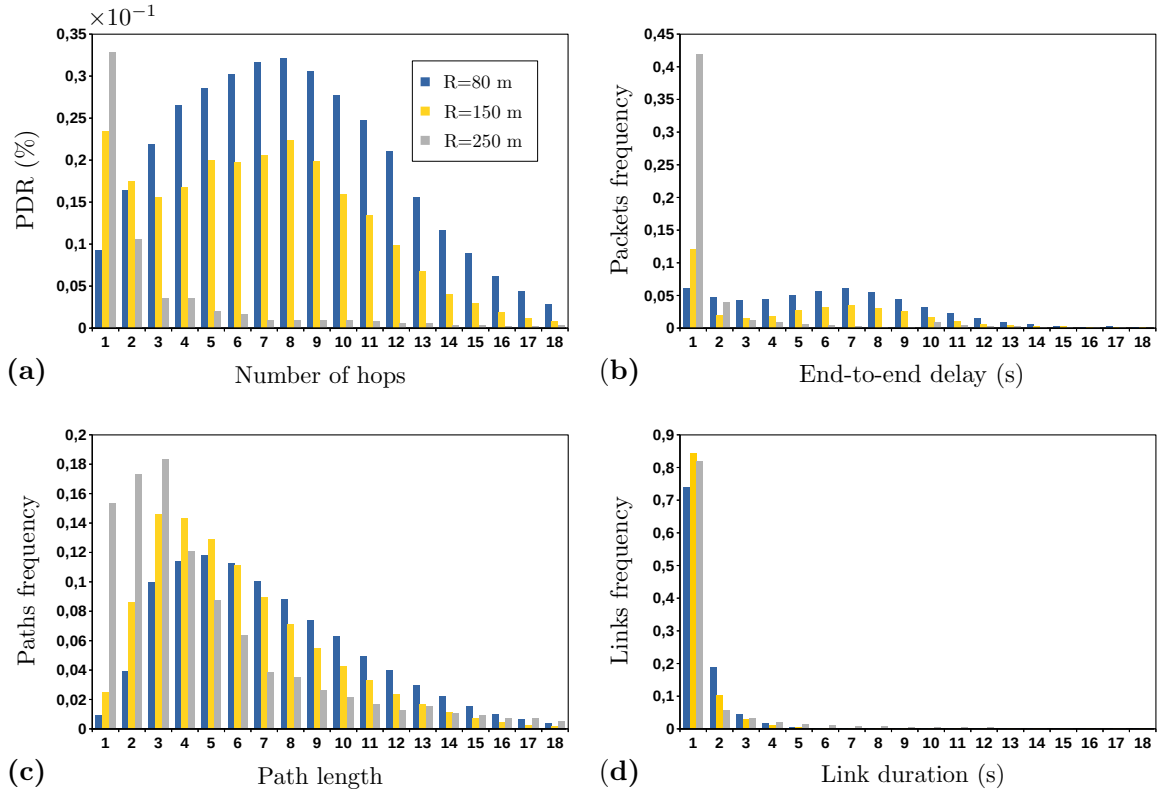

Fig. 18. Distribution of Packet delivery ratio (a), End-to-end delay (b), Path length (c), and Link duration (d) with high network density and varying transmission radius (R = 250 m, R = 150 m, and R = 80 m). The used mobility model is BA-Realtime, network density is 320 $vehs/km^2$, maximum speed v_{max} = 81 km/h, the number of RSUs is 10.

Fig. 18a shows that the packet delivery ratio as a function of the number of hops under high network density is increased as the network density is increased (see Fig. 17a for comparison). This is because vehicles are able to establish long paths as the network density is higher enough (i.e. 320 $vehs/km^2$) (see Fig. 18c).

Furthermore, Fig. 18a and Fig. 18c show that both the packet delivery ratio and paths length decrease significantly when the transmission range increases. We can explain that by the fact that the increase in the transmission range has a significant impact on the stability of established paths, but at the same time, this has a worse impact on the accessibility to the channel as it becomes congested. Thus, a much higher number of packets will be lost just because the queue is saturated as there is no available established path with the destination. On the other hand, when the transmission range is decreased, we observed an increase in paths length due to the increase in the network density. However, an increase in the end-to-end delay is observed due to high queueing delay at relay nodes and an extra delay caused by the route recovery process in the case of link break (see Fig. 18d). Regardless of that, under a low transmission range, the network shows a better performance in terms of packet delivery ratio (see Fig. 18c).

5.3. The effect of RSUs deployment strategy

In this section, we analyze both the network performance and connectivity condition based on a RSUs deployment strategy in terms of RSUs' position and number (see Fig. 12). Accordingly, the number of RSUs varies into $\{10, 30, 40, 50\}$ and the position of RSUs is determined based on the approach described in Fig. 12. The transmission range, mobility model, and maximum speed are fixed to 80 m, BA-Realtime, and 81 km/h, respectively. First, we analyze the network reliability and connectivity condition according to several performance metrics, including packet delivery ratio, paths length, link duration, and end-to-end delay, while varying the network density of vehicles and both the number and position of RSUs, respectively (see Fig. 19).

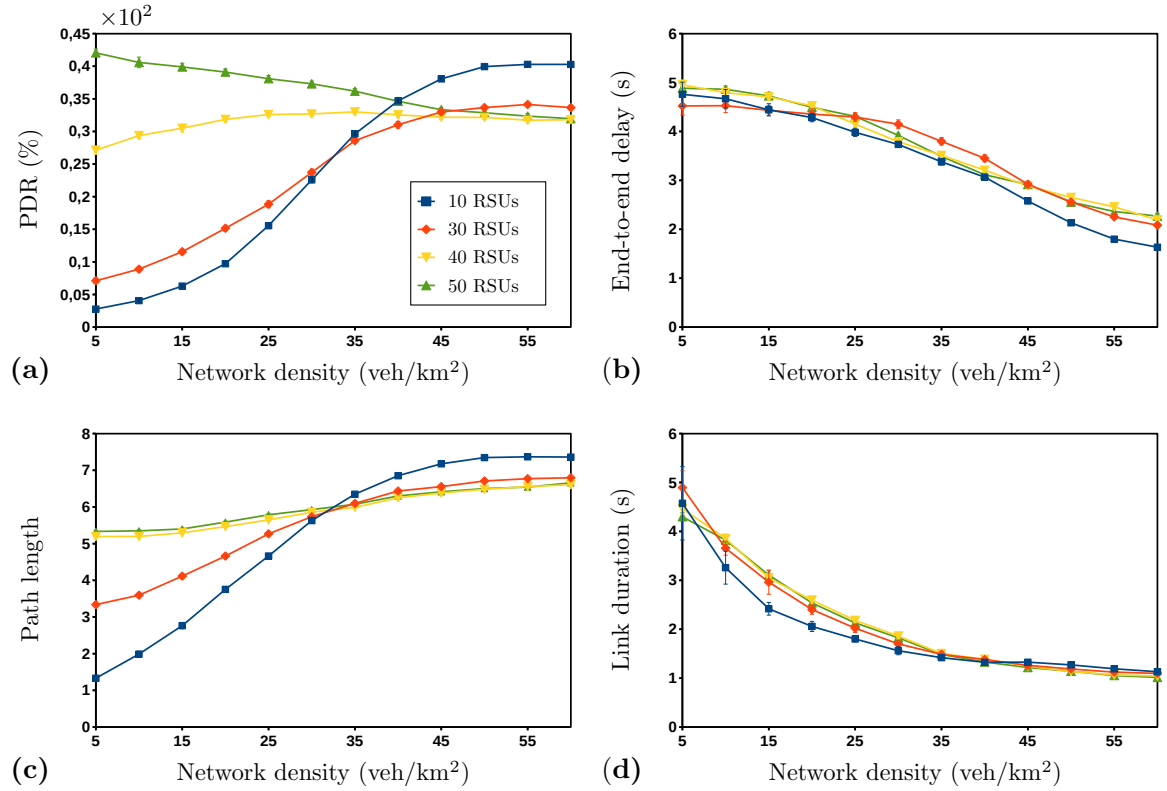

Fig. 19. Effect of increasing the network density with varying number of RSUs (10, 30, 40, and 50): (a) Packet delivery ratio, (b) End-to-end delay, (c) Path length, and (d) Link duration. The used mobility model is BA-Realtime, maximum speed $v_{max} = 81$ km/h and transmission range R = 80 m.

Second, we analyze the network reliability and connectivity condition based on the distributions of packet delivery ratio, end-to-end delay, link duration, and path length, while varying both the number and position

of RSUs. The network density N is fixed to 60 $vehs/km^2$ (see Fig. 20), firstly, and then, is fixed to 120 $vehs/km^2$ (see Fig. 21).

Fig. 19 shows that the RSUs number can improve very significantly the performance of the network in terms of packet delivery ratio as well as a function of network density except for a higher RSUs' number (i.e., 50 RSUs). Moreover, under the highest number of deployed RSUs, it is observed that the packet delivery ratio decreases slightly as a function of network density. The higher increase in the network density combined with a higher number of RSUs may lead to an increase in coverage level and the stability of established paths as a considerable number of RSUs participate in these paths. This is expected to result in a congested channel, and therefore this will cause data loss due to saturated queues at sender nodes (see Fig. 19c). On the other hand, under a low number of deployed RSUs (i.e., 10 RSUs), it is observed that the packet delivery ratio increase as a function of network density due to an increase in the connectivity level between vehicles. Fig. 19b shows that the end-to-end delay decreases as a function of network density, but a higher number of RSUs (30, 40, and 50) causes an increase in the end-to-end delay. This means that the increase in the end-to-end delay is expected to be related to an increase in the network overhead, the higher the number of RSUs, the higher the end-to-end delay.

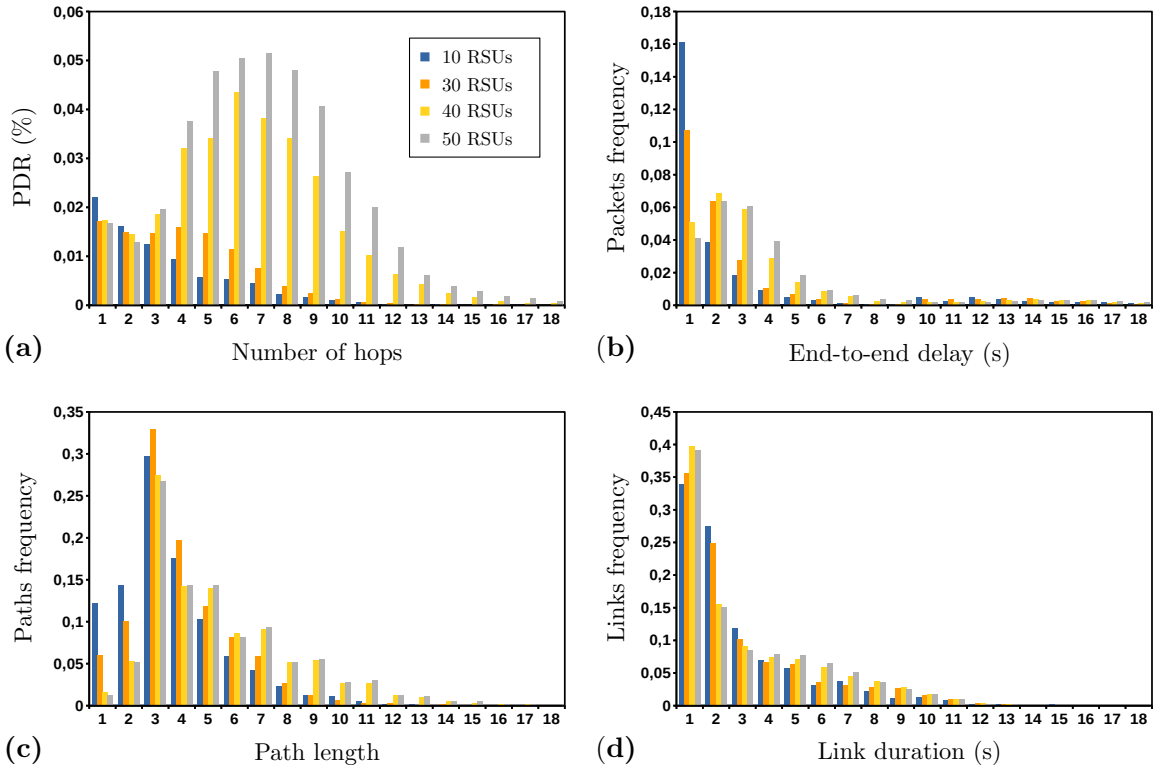

Fig. 20. Distribution of Packet delivery ratio (a), End-to-end delay (b), Path length (c), and Link duration (d) with low network density and varying number of RSUs (10, 30, 40, and 50). The used mobility model is BA-Realtime, maximum speed v_{max} = 81 km/h, transmission range R = 80 m and network density is 60 $vehs/km^2$.

By comparing the results of both Fig. 20 and Fig. 21 in terms of packet delivery ratio, average end-to-end, path length, and link duration delay under two different network densities (60 $vehs/km^2$ and 120 $vehs/km^2$) and varying number of deployed RSUs (10, 30, 40 and 50), we can observe that the packet delivery ratio as a function of the number of hops under low network density increases while increasing the number of deployed RSUs. It is also observed that when the number of deployed RSUs increases, the packets are received at a high number of hops. This is because vehicles can establish long paths profiting from stable wireless links with RSUs and higher network density (see Fig. 20c and Fig. 21c). However, it is observed that the longer

the established paths, the lower the link duration. Because a long-established path is susceptible to link break, and therefore all related links to this path will fail due to the propagation of an error message.

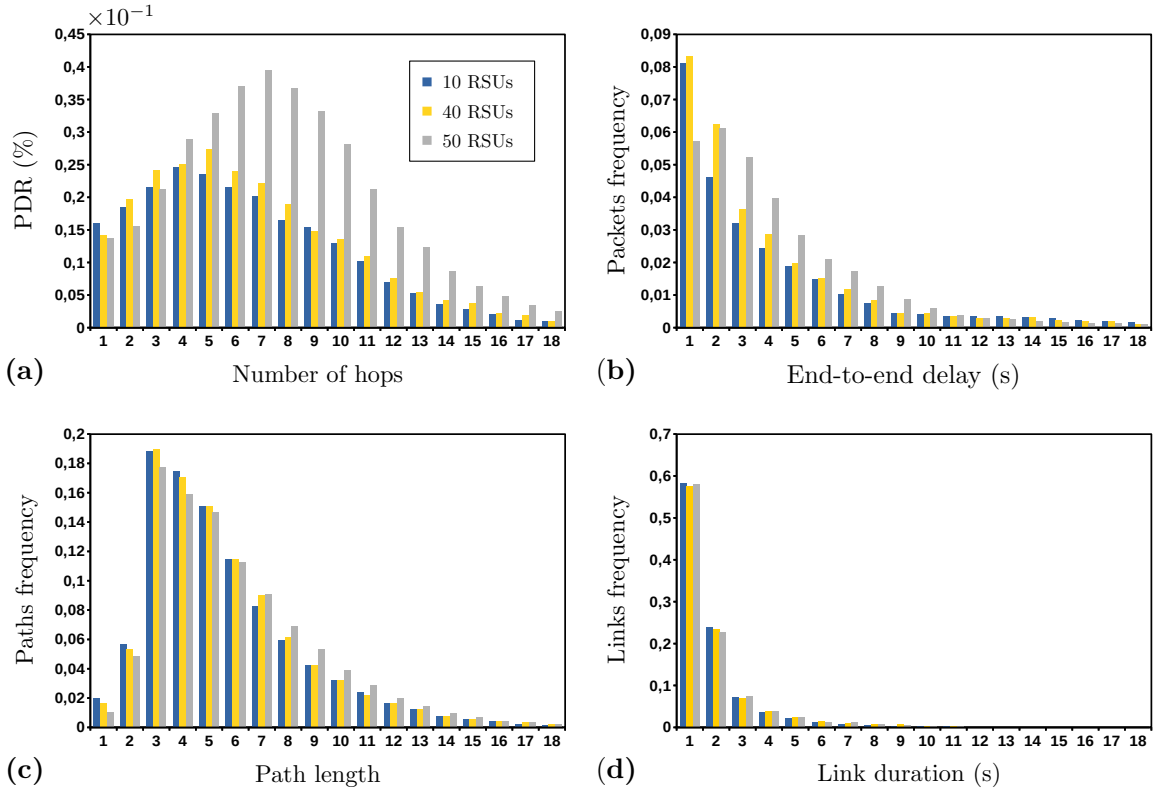

Fig. 21. Distribution of Packet delivery ratio (a), End-to-end delay (b), Path length (c), and Link duration (d) with high network density and varying number of RSUs (10, 30, 40, and 50). The used mobility model is BA-Realtime, maximum speed v_{max} = 81 km/h (cells/s), transmission range R = 80 m and network density is 120 $vehs/km^2$.

Under the lowest number of deployed RSUs (i.e., 10 RSUs) and low network density (60 $vehs/km^2$), we can see that the established paths are almost short due to a low connectivity level (see Fig. 20c). Accordingly, a high ratio of packets are received at a short number of hops (see Fig. 20a). On the other hand, the number of deployed RSUs has a significant impact on the end-to-end delay, where a higher number of RSUs can increase the end-to-end as it allows vehicles to establish long paths. This means that a considerable proportion of packets could be received at a high number of hops. In contrast, under the lowest number of deployed RSUs and network density, the established paths are relatively short, and therefore the sent packets can reach the destination very quickly as the number of relay nodes is small which results in a decreased end-to-end delay (see Fig. 20b).

Fig. 21a shows that when the network density is increased (120 $vehs/km^2$), the packet delivery ratio is significantly increased and the frequency of the established paths is significantly decreased causing a decrease in wireless links frequency (see Fig. 21c–d). This can be explained by the fact that the increase in the network density can improve the network connectivity, and thus the established paths become more stable and short. Fig. 21b shows that the end-to-end delay increases as the number of RSUs decreases due to the fact that vehicles are able to establish long paths, and therefore this leads to an additional delay caused by queueing process at relay nodes in the case of link failure. On the other hand, Fig. 21c shows that the path length is the same regardless of RSUs' number except for 50 RSUs, where a slight increase in the frequency of long paths is observed. This can be explained by the fact that the increased number of RSUs allows the establishment of relatively stable paths, especially when multiple RSUs are part of established

paths.

5.4. Analysis of link failure due to turning movements

In this section, we analyze extensively the link failures in terms of link duration and the last cause of link break. Accordingly, the network density of vehicles is fixed to N = 80 $vehs/km^2$ (see Fig. 22a–b), firstly, and then, is fixed to N = 360 $vehs/km^2$ (see Fig. 22c–d). The maximum speed is fixed to v_{max} = 81 km/h (see Fig. 22a–c), firstly, and then, is fixed to v_{max} = 135 km/h (see Fig. 22b–d). The transmission range and mobility model are fixed to 80 m and BA-Realtime, respectively. The simulation results are depicted in terms of the distributions of link duration and the last cause of wireless link break in the case of vehicle turning and without vehicle turning. In the case of link break without vehicle turning, three classifications of moving vehicles direction are introduced, including vehicles moving in the same direction, vehicles moving in the opposite direction, and vehicles moving in the perpendicular direction.

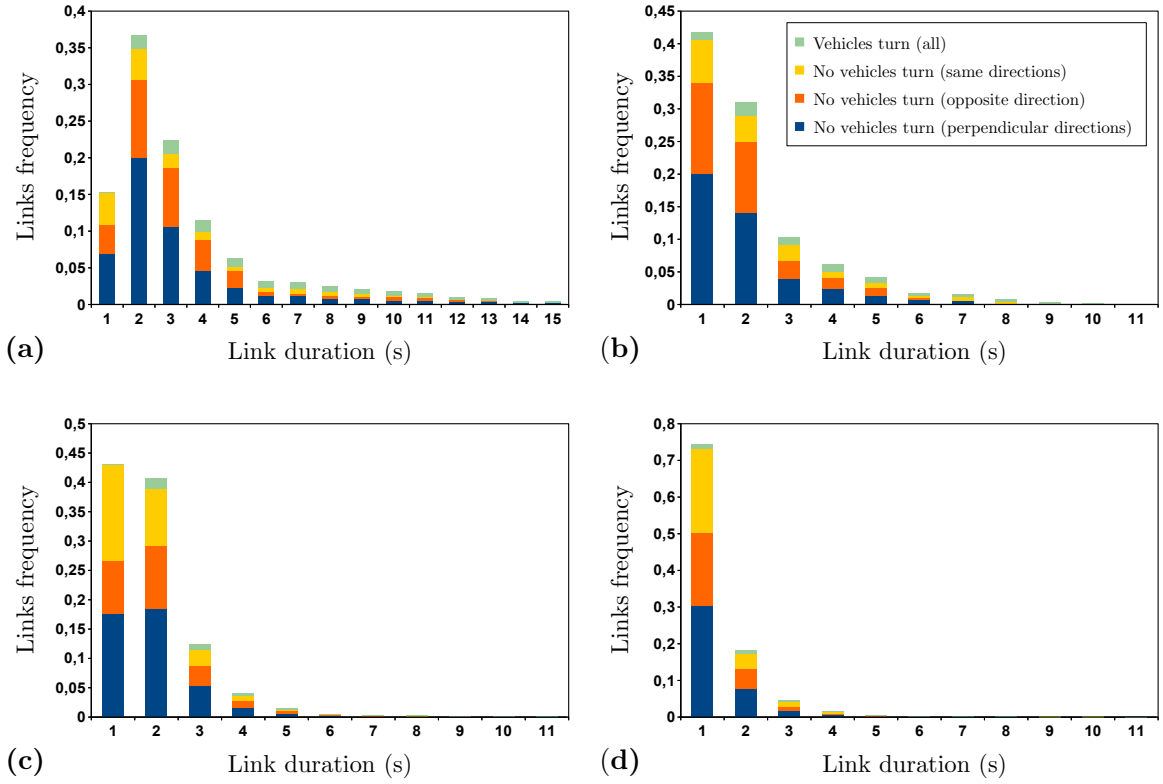

Fig. 22. Distribution of link duration with varying network density and maximum speed: (a) N = 80 $vehs/km^2$ and v_{max} = 81 km/h, (b) N = 80 $vehs/km^2$ and v_{max} = 135 km/h, (c) N = 360 $vehs/km^2$ and v_{max} = 81 km/h, and (d) N = 360 $vehs/km^2$ and v_{max} = 135 km/h. The used mobility model is BA-Realtime, transmission range R = 80 m and the number of RSUs is 0.

Fig. 22a shows that under low network density (80 $vehs/km^2$) and maximum speed (v_{max} = 81 km/h) respectively, most of the link failures occur with no vehicles turn within the time interval [1, 4]. We can explain that by the fact that when two vehicles A and B travel in perpendicular or opposite movement' directions, the distance between them increases rapidly, causing an early link failure (see Fig. 11a–b). For link failures related to the movement of vehicles in the same direction, this can occur in the case of two vehicles A and B that are moving at different speeds; however, this includes two main scenarios: (1) A is a preceding vehicle and B is a following vehicle, and (2) A is a preceding vehicle and B is not the following vehicle (see Fig. 11c). On the other hand, in the time interval [5,15], it is observed that link failures due to the turning of vehicles are more significant as compared with other scenarios. This means that unexpected

turning of vehicles at roundabouts is among the main factor responsible for link failures for established paths with long lifetime and this in turn means that the other causes of link breaks are the most frequent.

Fig. 22b shows that the link failures are significantly affected by the increase in the vehicles' maximum speed, where a high proportion of link failures with a long lifetime are disappeared. Moreover, a high rate of link failures is observed within the time interval [0, 1] as compared with the results in Fig. 22a. We can explain that by the increase in the vehicles' speed which causes a drastic change in the inter-vehicular distance regardless of the movement direction of vehicles. Therefore, this confirms that an increase in the vehicles' speed may amplify the rate of link failures.

When the network density is increased significantly (360 $vehs/km^2$), it is observed that most link failures are characterized by a short lifetime. This is expected to be due to the ability of vehicles to establish long paths under an increased network density, and therefore these paths are more susceptible to link failures (see Fig. 22c).

Fig. 22d shows that under both high network density (360 $vehs/km^2$) and maximum speed ($v_{max} = 135$ km/h), respectively, the link failures highly increases. This is mainly due to an increase in the vehicles' speed which amplifies the link failures, and therefore the established paths become extensively susceptible to link break. In other words, the vehicle's speed and network density are the key factors responsible for link failures.

6. Conclusion

In this paper, the network performance and the connectivity characteristics in a large-scale VANET scenario have been studied based on three realistic mobility models. The first one is capable of providing real-time path planning for vehicles between a pair of origin–destination based on a shortest path algorithm. The second mobility model provides a path planning for vehicles without a periodic update versus time (i.e., vehicles keep the same paths until they reach the destination). Based on the proposed mobility models, we first evaluated the traffic system according to various performance metrics to capture interesting mobility characteristics in terms of traffic flow, average speed, and travel time. Secondly, we extensively analyzed the network performance and connectivity dynamics based on various effective factors, including mobility model, transmission range, vehicles speed, vehicles density, and RSUs deployment strategy. For this purpose, we considered several performance metrics, including packet delivery ratio, end-to-end delay, path length, and link duration.

The simulation results show that the real-time planning of vehicles' trajectories helps in improving significantly the traffic state. On the other hand, traffic lights have a significant impact on the traffic state. Secondly, network simulation results show that the network performance is more sensitive to all factors noticed above. Accordingly, under low vehicles density, the link duration, the stability of paths, and the network reliability could be improved if the number of RSUs or the transmission range is increased and vice versa. Under higher vehicles' density, small transmission ranges can be considered better in the case of high network density regardless that packets are received at a higher number of hops. Moreover, the link duration (resp. established paths lifetime) and network reliability could be improved when the number of RSUs is increased. Finally, simulation results show that the links' duration is affected by unexpected turning of vehicles at intersections (roundabouts) and highly affected when the moving direction of both vehicles is perpendicular, opposite or vehicles move in the same direction. Future work may include different traffic scenarios to analyze the network connectivity; proposing solutions to increase links' duration; optimizing RSUs deployment strategy.

References

[1] A. Moubayed, A. Shami, P. Heidari, A. Larabi, R. Brunner, Edge-enabled V2X service placement for intelligent transportation systems, IEEE Transactions on Mobile Computing 20 (4) (2020) 1380–1392.

[2] Z. Yang, L. S. Pun-Cheng, Vehicle detection in intelligent transportation systems and its applications under varying environments: A review, Image and Vision Computing 69 (2018) 143–154.

[3] M. Lee, T. Atkison, Vanet applications: Past, present, and future, Vehicular Communications 28 (2021) 100310.

[4] A. R. Khan, M. F. Jamlos, N. Osman, M. I. Ishak, F. Dzaharudin, Y. K. Yeow, K. A. Khairi, DSRC Technology in Vehicle-to-Vehicle (V2V) and Vehicle-to-Infrastructure (V2I) IoT System for Intelligent Transportation System (ITS): A Review, Recent Trends in Mechatronics Towards Industry 4.0 (2022) 97–106.
[5] H. Zhang, L. Wei, Topology characteristic analysis of vehicular ad hoc network based on time-varying complex network, AIP Advances 11 (11) (2021) 115011.
[6] S. Grozdanov, On the connection between hydrodynamics and quantum chaos in holographic theories with stringy corrections, Journal of High Energy Physics 2019 (1) (2019) 1–21.
[7] M. Zarei, Traffic-centric mesoscopic analysis of connectivity in VANETs, The Computer Journal 63 (2) (2020) 203–219.
[8] F. A. Silva, A. Boukerche, T. R. Silva, L. B. Ruiz, A. A. Loureiro, A novel macroscopic mobility model for vehicular networks, Computer Networks 79 (2015) 188–202.
[9] Z. Cai, M. Liang, Q. Sun, MMIR: a microscopic mechanism for street selection based on intersection records in urban VANET routing, EURASIP Journal on Wireless Communications and Networking 2019 (1) (2019) 1–15.
[10] J. Naskath, B. Paramasivan, H. Aldabbas, A study on modeling vehicles mobility with MLC for enhancing vehicle-to-vehicle connectivity in VANET, Journal of Ambient Intelligence and Humanized Computing 12 (8) (2021) 8255–8264.
[11] D. Naboulsi, M. Fiore, Characterizing the instantaneous connectivity of large-scale urban vehicular networks, IEEE Transactions on Mobile Computing 16 (5) (2016) 1272–1286.
[12] C. Miao, H. Liu, G. G. Zhu, H. Chen, Connectivity-based optimization of vehicle route and speed for improved fuel economy, Transportation Research Part C: Emerging Technologies 91 (2018) 353–368.
[13] T. Shanmukhappa, et al., Spatial analysis of public transport network from a complex network perspective and its impact on vehicular network connectivity .
[14] M. Kezia, K. Anusuya, Mobility Models for Internet of Vehicles: A Survey, Wireless Personal Communications (2022) 1–25.
[15] H. Xiao, Q. Zhang, S. Ouyang, A. T. Chronopoulos, Connectivity probability analysis for VANET freeway traffic using a cell transmission model, IEEE Systems Journal 15 (2) (2020) 1815–1824.
[16] N. Akhtar, S. C. Ergen, O. Ozkasap, Vehicle mobility and communication channel models for realistic and efficient highway VANET simulation, IEEE Transactions on Vehicular Technology 64 (1) (2014) 248–262.
[17] L. Bedogni, M. Fiore, C. Glacet, Temporal reachability in vehicular networks, in: IEEE INFOCOM 2018-IEEE Conference on Computer Communications, IEEE, 81–89, 2018.
[18] X. Hou, Y. Li, D. Jin, D. O. Wu, S. Chen, Modeling the Impact of Mobility on the Connectivity of Vehicular Networks in Large-Scale Urban Environments, IEEE TRANSACTIONS ON VEHICULAR TECHNOLOGY 65 (4) (2016) 2753.
[19] J. Cheng, H. Mi, Z. Huang, S. Gao, D. Zang, C. Liu, Connectivity modeling and analysis for internet of vehicles in urban road scene, IEEE Access 6 (2017) 2692–2702.
[20] C. Guo, D. Li, G. Zhang, M. Zhai, Real-time path planning in urban area via vanet-assisted traffic information sharing, IEEE Transactions on Vehicular Technology 67 (7) (2018) 5635–5649.
[21] L. Cheng, E. Verbeek, P. S. Skardal, A Preliminary Study on the VANET Topology Characteristics from Propagation-Aware Traffic Flows Extracted from Measured Data, in: 2020 IEEE International Symposium on Antennas and Propagation and North American Radio Science Meeting, IEEE, 1161–1162, 2020.
[22] P. Barbecho Bautista, L. Urquiza-Aguiar, M. Aguilar Igartua, Evaluation of dynamic route planning impact on vehicular communications with SUMO, in: Proceedings of the 23rd International ACM Conference on Modeling, Analysis and Simulation of Wireless and Mobile Systems, 27–35, 2020.
[23] M. A. Salman, F. S. Mubarek, N. I. Seno, Effect of Traffic Light Scenario on VANETs Connectivity with Low Penetration Rate, Journal of Southwest Jiaotong University 54 (3).
[24] F. Li, W. Chen, Y. Shui, J. Wang, K. Yang, L. Xu, J. Yu, C. Li, Connectivity probability analysis of VANETs at different traffic densities using measured data at 5.9 GHz, Physical Communication 35 (2019) 100709.
[25] Z. Khan, P. Fan, S. Fang, On the connectivity of vehicular ad hoc network under various mobility scenarios, IEEE Access 5 (2017) 22559–22565.
[26] O. Rehman, R. Qureshi, M. Ould-Khaoua, M. F. Niazi, Analysis of mobility speed impact on end-to-end communication performance in VANETs, Vehicular Communications 26 (2020) 100278.
[27] M. Wilsher, C. P. Dettmann, A. Ganesh, Connectivity in one-dimensional soft random geometric graphs, Physical Review E 102 (6) (2020) 062312.
[28] S. Elaraby, S. M. Abuelenin, Connectivity analysis of directed highway vehicular ad hoc networks using graph theory, International Journal of Communication Systems 34 (5) (2021) e4745.
[29] B. Yelure, et al., Analysis of Connectivity Duration In Vehicular Network, Turkish Journal of Computer and Mathematics Education (TURCOMAT) 12 (13) (2021) 2318–2325.
[30] X. Li, R. Zhou, T. Zhou, L. Liu, K. Yu, Connectivity Probability Analysis for Green Cooperative Cognitive Vehicular Networks, IEEE Transactions on Green Communications and Networking .
[31] O. E. Joubari, J. B. Othman, V. Vèque, Markov Chain Mobility Model for Multi-lane Highways, Mobile Networks and Applications (2022) 1–13.
[32] J. Zhang, Z. Lin, Multi-hop connectivity analysis and RSU deployment in urban vehicular networks, in: International Conference on Intelligent Traffic Systems and Smart City (ITSSC 2021), vol. 12165, SPIE, 597–609, 2022.
[33] A. Ilyés, T. Kovács, G. Tisza, I. Varga, Spatial Characteristics of Communication in Urban Vehicular System., in: COMPLEXIS, 108–112, 2020.
[34] D. Ziegler, J. Betz, M. Lienkamp, Unified Mobility Estimation Model, in: 2021 IEEE International Intelligent Transportation Systems Conference (ITSC), IEEE, 3610–3617, 2021.
[35] C. Celes, F. A. Silva, A. Boukerche, R. M. de Castro Andrade, A. A. Loureiro, Improving vanet simulation with calibrated

vehicular mobility traces, IEEE Transactions on Mobile Computing 16 (12) (2017) 3376–3389.
[36] B. Pan, H. Wu, Performance analysis of connectivity considering user behavior in V2V and V2I communication systems, in: 2017 IEEE 86th Vehicular Technology Conference (VTC-Fall), IEEE, 1–5, 2017.
[37] K. Nagel, M. Schreckenberg, A cellular automaton model for freeway traffic, Journal de physique I 2 (12) (1992) 2221–2229.
[38] M. Parimala, S. Broumi, K. Prakash, S. Topal, Bellman–Ford algorithm for solving shortest path problem of a network under picture fuzzy environment, Complex & Intelligent Systems 7 (5) (2021) 2373–2381.
[39] K. Han, T. Yao, C. Jiang, T. L. Friesz, Lagrangian-based hydrodynamic model for traffic data fusion on freeways, Networks and spatial economics 17 (4) (2017) 1071–1094.
[40] J. Zeng, Y. Qian, F. Yin, L. Zhu, D. Xu, A multi-value cellular automata model for multi-lane traffic flow under lagrange coordinate, Computational and Mathematical Organization Theory (2021) 1–15.
[41] Y. Regragui, N. Moussa, A cellular automata model for urban traffic with multiple roundabouts, Chinese journal of physics 56 (3) (2018) 1273–1285.